

Lawrence Berkeley National Laboratory

Lawrence Berkeley National Laboratory

Title

What product might a renewal of Heavy Ion Fusion development offer that competes with methane microbes and hydrogen HTGRs

Permalink

<https://escholarship.org/uc/item/6tv2m11x>

Authors

Logan, Grant

Lee, Ed

Yu, Simon

et al.

Publication Date

2006-04-19

What product might a renewal of Heavy Ion Fusion development offer that competes with methane microbes and hydrogen HTGRs?

Grant Logan, with acknowledgment of collaborators: Ed Lee, Simon Yu, Dick Briggs, John Barnard, Alex Friedman, Hong Qin, Will Waldron, Mattaheus Leitner, Joe Kwan, Enrique Henestroza, George Caporaso, Wayne Meier, Max Tabak, Debbie Callahan, Ralph Moir, and Per Peterson
(May 1, 2006 Progress Report)

In 1994 a Fusion Technology journal publication by Logan, Moir and Hoffman described how exploiting unusually-strong economy-of-scale for large (8 GWe-scale) multi-unit HIF plants sharing a driver and target factory among several low cost molten salt fusion chambers @ < \$40M per 2.4 GW fusion each (Fig. 1), *could produce electricity below 3 cts/kWehr, even lower than similar multi-unit fission plants*. The fusion electric plant could cost \$12.5 B for 7.5 GWe and produce hydrogen fuel by electrolysis at prices competitive with gasoline-powered hybrids getting fuel from oil at \$20\$/bbl. At \$60/bbl oil, the fusion plant can cost \$35B and compete @ 10% APR financing.

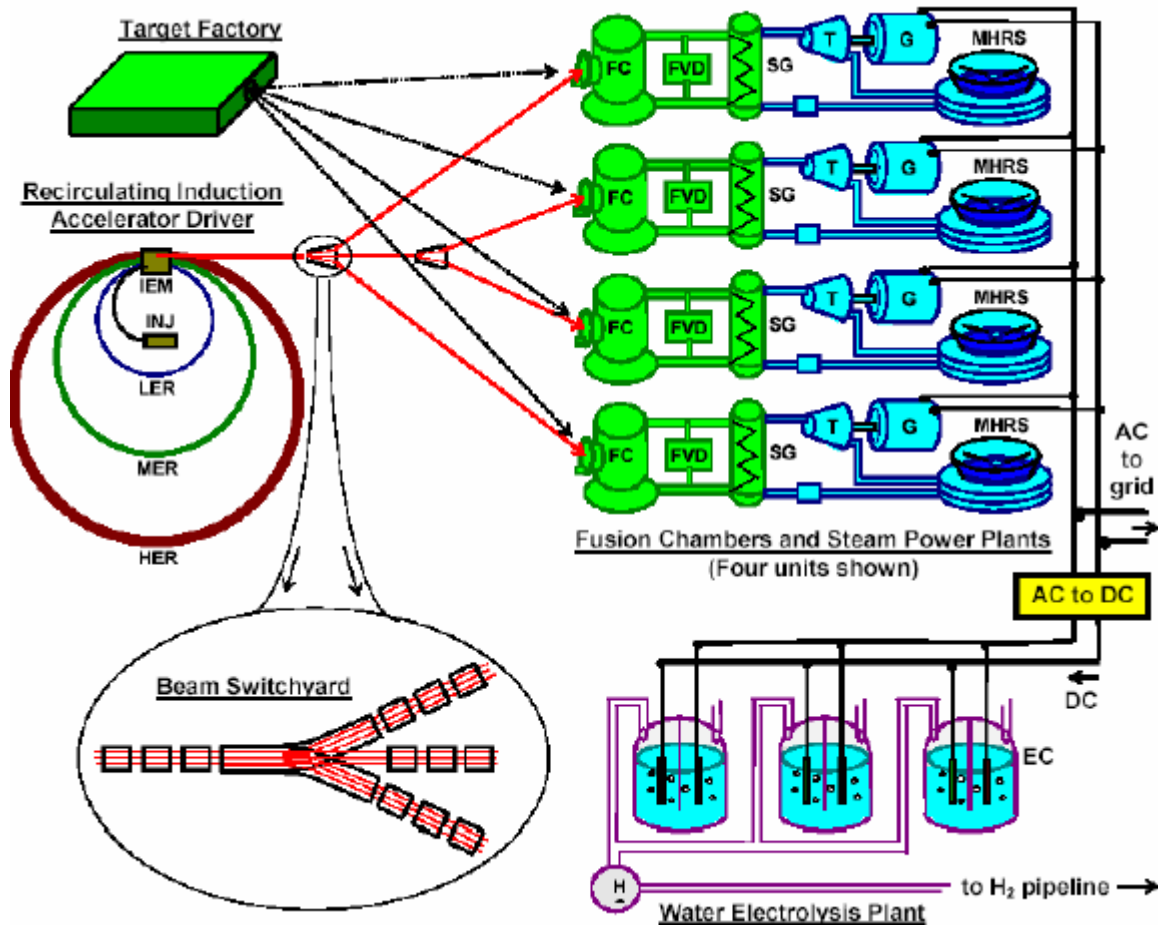


Figure 1: 1994 concept for a large multi-unit heavy ion fusion plant producing hydrogen.

Given massive and still-increasing world demand for transportation fuel even with oil climbing above \$60/bbl, large HIF plants producing both low cost electricity and hydrogen could be more relevant to motivate new R&D funding for HIF development in the next few years. Three major challenges to get there: (1) *NIF ignition in indirect drive geometry for liquid chambers*, (2) *a modular accelerator to enable a one-module IRE < \$100 M*, (3) *compatible HIF target, driver and chamber allowing a small driver @ < \$500 M cost for a >100MWe net power DEMO.*

-->Need to demo small before growing large.

This scoping study, at a very preliminary conceptual level, attempts to identify how we might meet the last two great challenges taking advantage of several recent ideas and advances which motivate reconsideration of modular HIF drivers: >60X longitudinal compression of neutralized ion beams using a variable waveform induction module in NDCX down to 2 nanosecond bunches, the proof-of-principle demonstration of fast optical-gated solid state SiC switches by George Caporaso's group at LLNL (see George's RPIA06 paper), and recent work by Ed Lee, John Barnard and Hong Qin on methods for time-dependent correction of chromatic focusing errors in neutralized beams with up to 10 % $\Delta v/v$ velocity tilt, allowing 5 or more bunches, and shorter bunches, and possibly < 1 mm radius focal spot targets. We seek multi-pulsing with neutralized compression and focusing to enable higher peak power capability and the ability to create nearly arbitrary composite "picket fence" pulse shapes can be used to innovate HIF target designs for lower driver energy, and at the same time, reduce unit driver cost per joule for given driver energy, and reduce development time. For example, Debbie Callahan has explored close-coupled HIF targets with adequate gains > 40 that would need higher peak beam intensities in order to reduce total driver energy below 1 MJ. In principle, both PLIA and induction accelerators might benefit from multiple short bunches (see June 24, 2005 talk by Logan on multi-pulsing in PLIA accelerators for IFE), although the PLIA approach, because of fixed circuit wave velocities at any z, requires imaginative work-arounds to handle the different bunch velocities required. George's RPIA06 paper also describes a different type of radial line induction linac that might be considered, but its unclear how the required pulse-to-pulse variable waveforms can be obtained with such pulselines. This initial MathCad analysis explores multi-pulsing in modular solenoid induction linacs (concept shown in Figure 1) considering high-q ECR sources, basic induction acceleration limits assuming affordable agile waveforms, transverse and longitudinal bunch confinement constraints, models to optimize bunch lengths, solenoid fields, core radial builds and switching. Figure 2 below illustrates one linac module for a driver example (not yet optimized) consisting of 40 linacs (20 at each end). Necessarily, this first look invokes many new ideas, but could they potentially meet the above challenges?

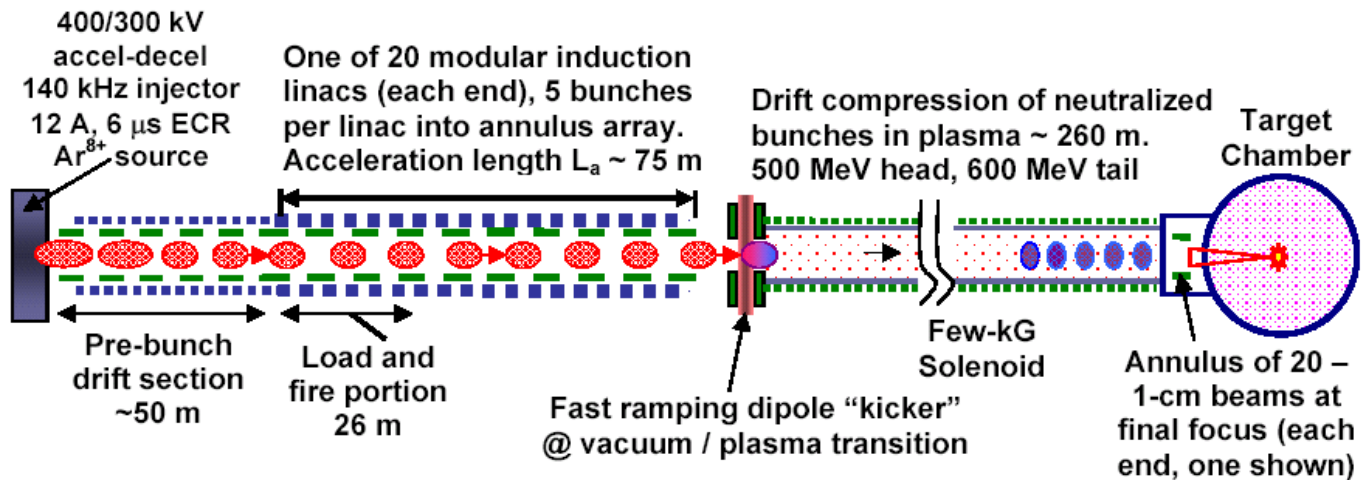


Figure 2. Concept for one of 40 modular induction linacs delivering a 1 MJ shaped pulse delivering up to 250 TW (@ 4ns) to 500 TW (@ 2ns) peak power, if needed, to drive close-coupled HIF targets for 40 MJ yields.

The concept depicted in Fig 1 calls for many new science and technology advances as discussed below, and so implies many new developments for this approach to a driver. On the other hand, the modular linac approach offers the possibility to reduce cost and schedule for HIF development, where one module can serve as an IRE. **We clearly need to address the HIF development path issue:** the best HIF development path we were able to present to FESAC in 2003 based on the IBX-->multiple-beam IRE-->RPD-type-ETF pathway was the longest development path of all MFE and IFE fusion approaches considered, even assuming then that HIF funding would grow to > \$100M/yr over 10 years. Some of the advances below are essential to enable a modular linac approach, such as neutralized compression to handle higher perveance beams for shorter linacs and fast, low cost GW switches, while others, such as higher magnetic fields, are not essential but maybe desirable on the assumption that future mass manufacturing costs will come down. **All advances, at least, should have plausible proof-of-principle feasibility, even if mature unit costs 30 years from now are not yet known.** The economics of microbe methane and HTGR hydrogen are also not known, but they are getting R&D funding attention right now. The strategy here is a motivational study to try to find out if our repertoire of innovations could make a "sufficient" difference to HIF attractiveness compared to current "new energy" R&D leaders. What "sufficient" is will ultimately be determined by competing energy technologies (which are improving) to be challenging us in the 30 year time frame. What "sufficient" means to convince notables such as the LBNL Director to support renewal of HIF is a related, more pressing question. If we can show credible physics and engineering fundamentals with an affordable development pathway to test the key issues, we can still motivate HIF renewal even if future reductions in manufacturing costs are required.

Many of the innovations listed below could in principle also be applied to multiple-beam quad drivers. In the fall of 2003, Wayne Meier and I used a modified systems code with common IBEAM cost models and unit costs to compare modular drivers (assuming NDC for all cases) for both quad and solenoid transport and for hybrids in-between. We found total driver costs per joule to be roughly the same within the cost model uncertainties. We'll need more time to re-consider all the mix and match possibilities with multi-pulsing. For now, we consider solenoid focusing for this study for three reasons (1) We expect competitive costs, even with 10 or more pulses, will still require **peak line-charge densities > 10 $\mu\text{C}/\text{m}$, and perveances > 10⁻² in the linac,** likely easier for solenoids to handle than quadrupoles. (2) We know that multiple beam quad drivers have a strong economic requirement for small bore, high fill factor, compact multiple-beam magnetic-quad arrays, which are likely to make e-cloud mitigation difficult. We need plausible e-cloud mitigation concepts to revisit those driver architectures. Conceptually, single beam solenoids with effective e-traps only at the ends should suffice to prevent electron ingress into the beam, although we have not yet experimentally confirmed effective e-traps on NDCX. We have an e-cloud experimental program on both HCX and NDCX, and new powerful simulation tools, that allow us to compare e-cloud mitigation techniques in both quadrupoles and solenoids, and we plan to pursue that research to validate any new driver designs. For now, solenoids appear to offer a more likely way to manage e-cloud effects in modular drivers, and we'll know soon enough. (3) Regardless of what path one might prefer for HIF driver development, we have to pursue warm dense matter physics opportunities now with very limited hardware budgets, and solenoid transport has been our lowest cost option to move forward with. This has a spin-off benefit of allowing us to experimentally evaluate some of the important physics associated with modular solenoid linac drivers in the near term. **Solenoids have been cheaper and faster to build for our HEDP program, and that should point to similar benefits for HIF development in the future.**

Ten innovations to be considered in this MathCAD study

(1) HIF target designs for lower yields requiring less than one MJ of total beam energy.

Our laser IFE competition that has continued with NNSA-HAPL money during the last few years have gained some attention in Washington for new approaches to an ETF-like facility that might produce repetitive fusion yields with less than **1 MJ** total driver energy, with driver costs under **\$0.5 B**. All of the modular solenoid cases we have considered recently appear to have accelerator efficiencies $\eta > 25\%$, so that only **40 MJ** fusion yields are needed for $\eta G > 10$. The figure below reproduced from Debbie Callahan and Max Tabak's PoP paper, vol 7, May 2000 "Progress in heavy ion fusion target design", show **gains $G > 40$ @ < 1 MJ driver energy.**

Phys. Plasmas, Vol. 7, No. 5, May 2000

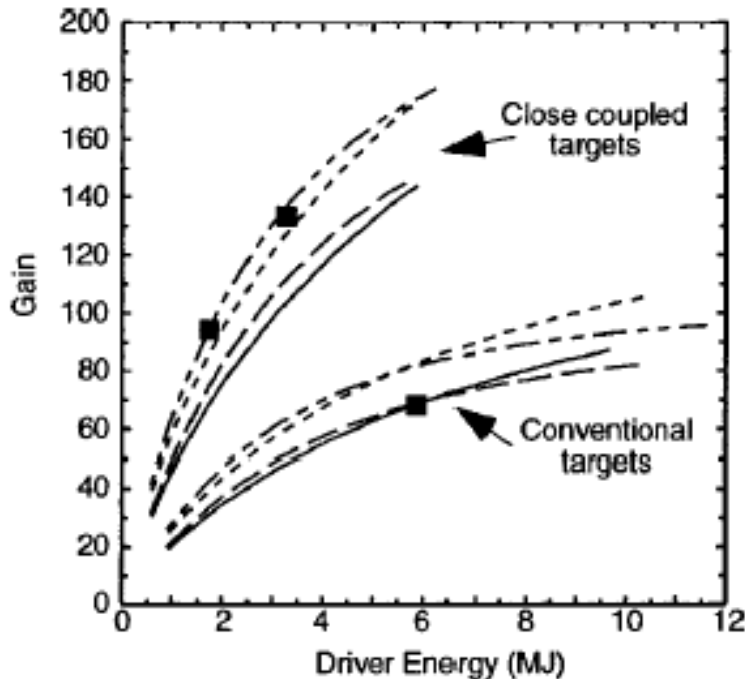


FIG. 11. Gain curves for the distributed radiator targets. The lower set of curves is for the conventional case-to-capsule ratio, while the upper set is for the close-coupled design. For each set, the solid curve is 250 eV drive and fixed ion range [i.e., converter densities are increased (decreased) as hohlraum length is shortened (lengthened)], the dashed curve is 250 eV drive and varying ion range [i.e., iron range is shortened (lengthened) as the hohlraum length is shortened (lengthened)], the dotted curve is 240 eV drive and fixed ion range, and the dot-dash curve is 240 eV drive and varying ion range. The squares represent the three integrated Lasnex calculation point designs.

Scaling up an accelerator and target pulse rate is the strongest way to decrease unit cost of electricity. Many fusion designers would say that 40 MJ yield with gains of 40, while acceptable for an ETF, would not make competitive CoE. While that would be true at 6 Hz (~ 100 MWe net output, it would be OK @ $\eta G > 10$ and @ 60 Hz for 1 GWe output, provided (a) target fab can be innovated to cost < nickel per target, and (b), the chamber is designed to clear at the speed of 1 eV plasma flow 2-3 km/s, rather than the speed of liquid droplets 20-30 m/s. (Fig.4)

Max Tabak has several other innovative target ideas $G > 40$ @ 1 MJ, provided flexible pulse shapes, small spots, and high peak powers are available.

Figure 3. Published HIF gain curves (Callahan, Tabak) show adequate gains > 40 for HIF targets at driver energies below 1 MJ-->also require focal spots ~ 0.7 mm radius. Such small spots will require smaller chambers and focal lengths consistent with low 40 MJ yields- Figure 3 below shows an example from a June 17, 2002 study.

(2) HIF chambers for small fusion yields, >50 Hz, and <1 meter final focus lengths.

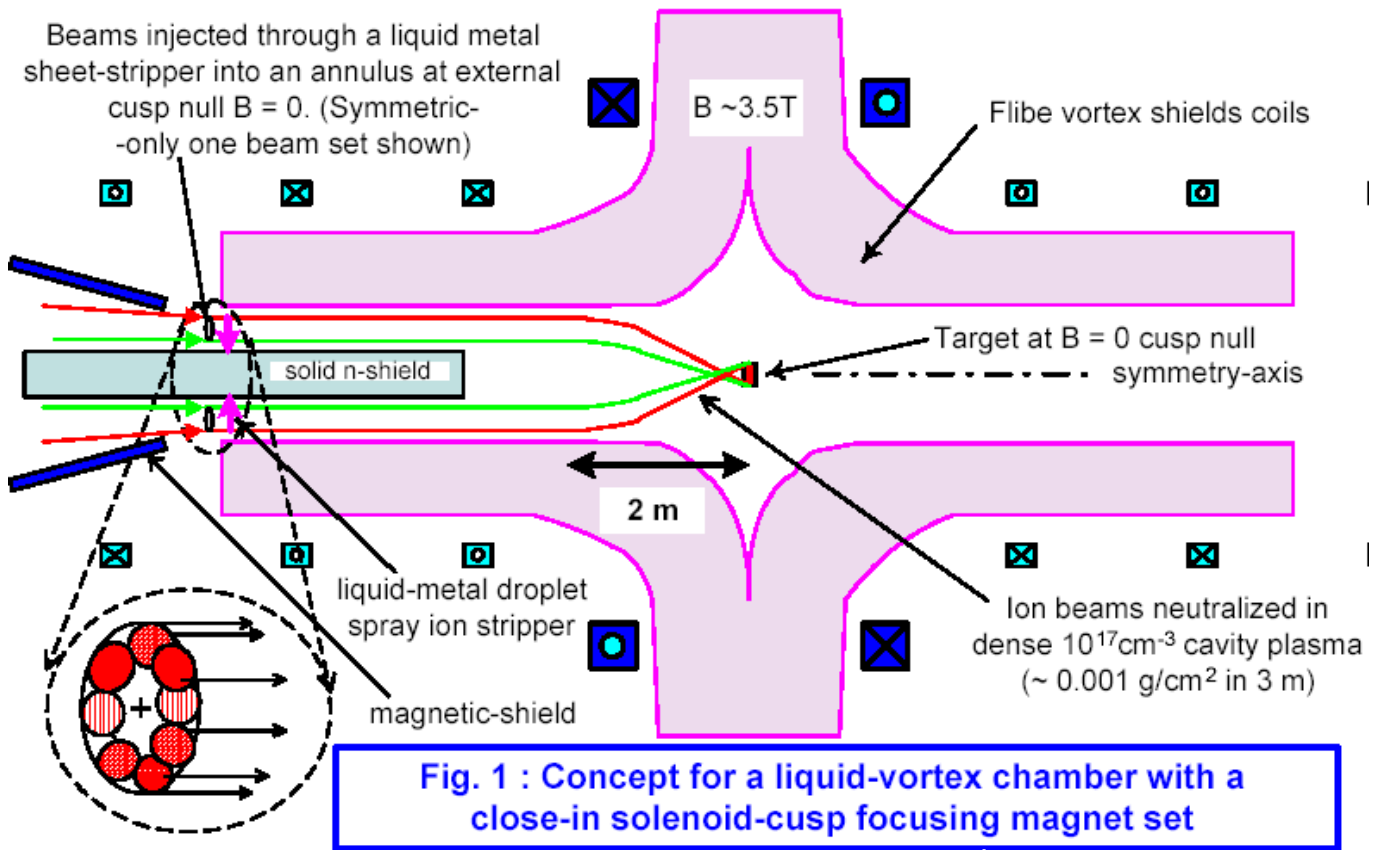
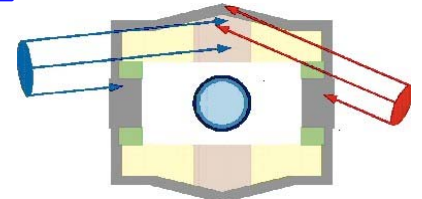


Figure 4: Example of a full size liquid Flibe vortex chamber reproduced from an unpublished June 17 2002 study by Logan for a 350 MJ fusion yield Distributed Radiator Target design. (Double-ended, only one end shown) For a 35 MJ yield (10 x smaller), roughly all dimensions would shrink by a factor of $10^{1/3} \sim 2.2$, except the Flibe layer thickness can shrink only ~20%. The net result would be an effective final focal length of only 1 m.



2002 DRT Target

Still, for multiple pulses with the tail pulse having 10% higher velocity than the first pulse, time dependent corrections are required to hit 0.7 mm radius beam spots on the close-coupled target radiator annulus. An upstream dipole kicker causes the last pulse to enter with a slightly steeper entrance angle than shown for the nominal head bunch, with smaller kicks for pulses in between the head and tail bunches. Figure 5 below shows conceptually how the time dependent focusing would apply to a single beam, e.g., for NDCX-II. Ed Lee presented a talk on this concept a couple months ago with some NDCX and driver examples. Ed Lee is currently developing an improved NDC-->FF-->Chamber example with time dependent focusing for an array of beams which point straight along an annular cone with very small convergence angle into a small (few cm radius circle entering the main chamber final focus-which will be a further optimization of the modular linac layout shown in Figure 5 next. **Tabak and Logan are planning to work on a variant of this chamber and target concept for plasma MHD direct conversion to reduce balance-of-plant costs (a la the old Compact Fusion Advanced Rankine Cycle scheme). Stay tuned.**

- (3) Modular solenoid linac driver architecture with beamlines arrayed around an annulus
- > Allows one module for an IRE --> faster development path
- > For a driver, annular beam array congruent with DRT target illumination geometry (Fig 4)
- > Cost saving by sharing pulsed power modules located along the axis

16 module solenoid driver (eight per end), total 6.7 MJ of 2.5 GeV Xe⁺⁸ ions, 7,000 tons of induction cores, \$250 M hardware, \$750 M total capital cost (See Sec. VI)

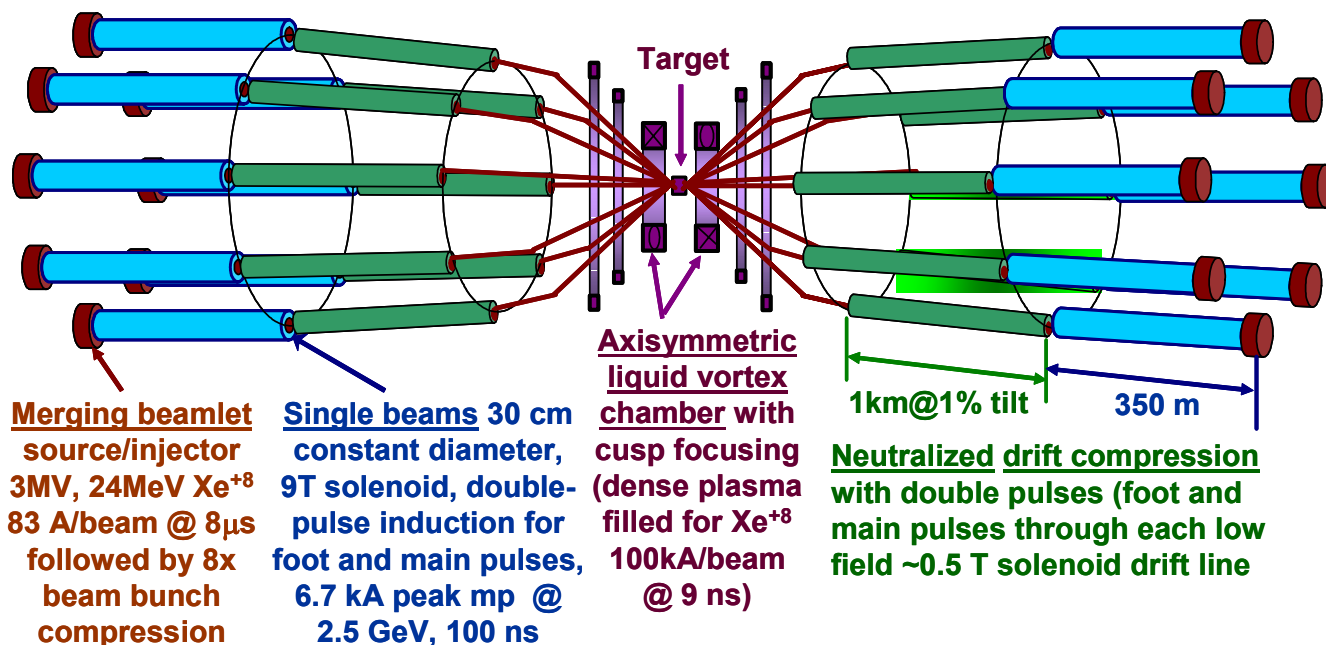


Figure 5. Concept for a modular solenoid linac driver system considered in an unpublished study January 29, 2003 (Grant Logan, Ed Lee, and Dick Briggs). This was sized to deliver single pulses of 6.7 MJ needed for 5 mm spot hybrid-DRT targets. Later, this case was revised to Ne⁺¹ for the summer study of 2003, finding a larger 24,000 tons of core mass.

In this new study, we assume time dependent corrections, < 1 mm spot targets @ < 1 MJ, with multi-pulsing of 5 or more bunches per linac, to reduce the radial size of each linac (smaller beam radius, solenoid radius, and core radius), compared to those needed in this earlier modular linac driver example.

(4) Time-dependent correction of chromatic aberrations with larger velocity tilts using NDC

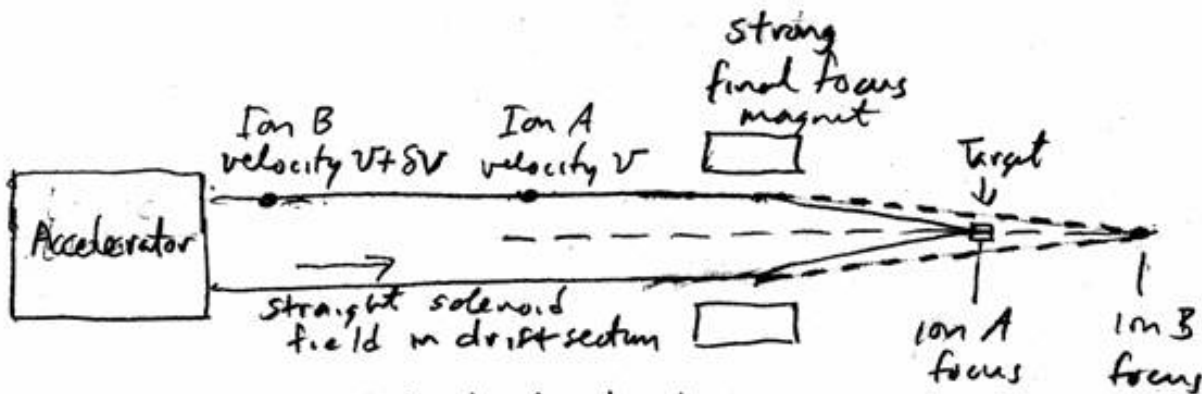


Fig. 1a Neutralized drift compression and focusing without time-dependent corrections

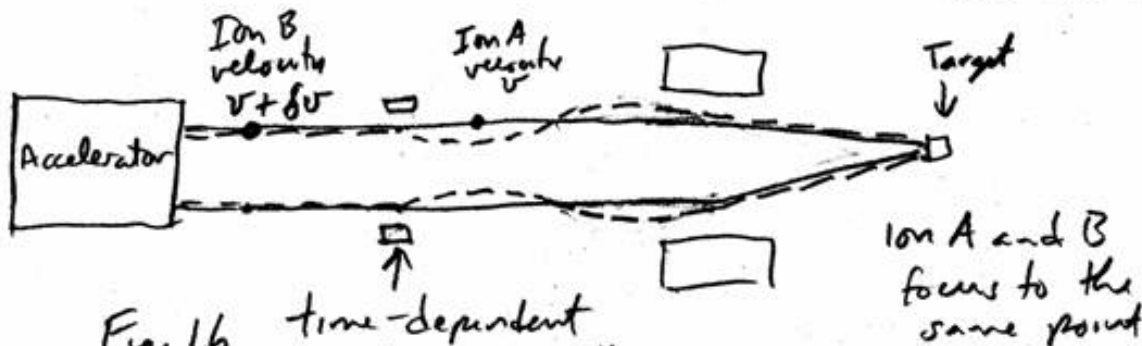


Fig. 1b time-dependent "kicker magnet" makes ion B undergo a radial oscillation so that faster ion B enters final focus at proper initial convergence angle

Figure 6 Concept for single beam time-dependent focusing to accommodate large velocity tilts. Equivalent approaches using fast ramping dipoles at the vacuum plasma NDC interfaces for multiple beams around an annulus is needed for 40 meter long multiple-pulse trains with 5 or more bunches. (Sketch by G. Logan, September 21, 2005)

Will Waldron has done a study "Time Dependent Final Focusing Element for NDCX-II Proposal" (Dec. 1, 2004), which shows a driver capability for any variant of kickers we are likely to need. Within a year, the LLNL Beam Research Program will demonstrate a four pulse kicker with 20 ns rise time in slicing up the DARHT-II kA electron beam at LANL.

(5) Agile waveform ear and tilt control capability to support multi-pulsing: manage bunches separately until arrival at a target in any prescribed "picket fence" pulse shape

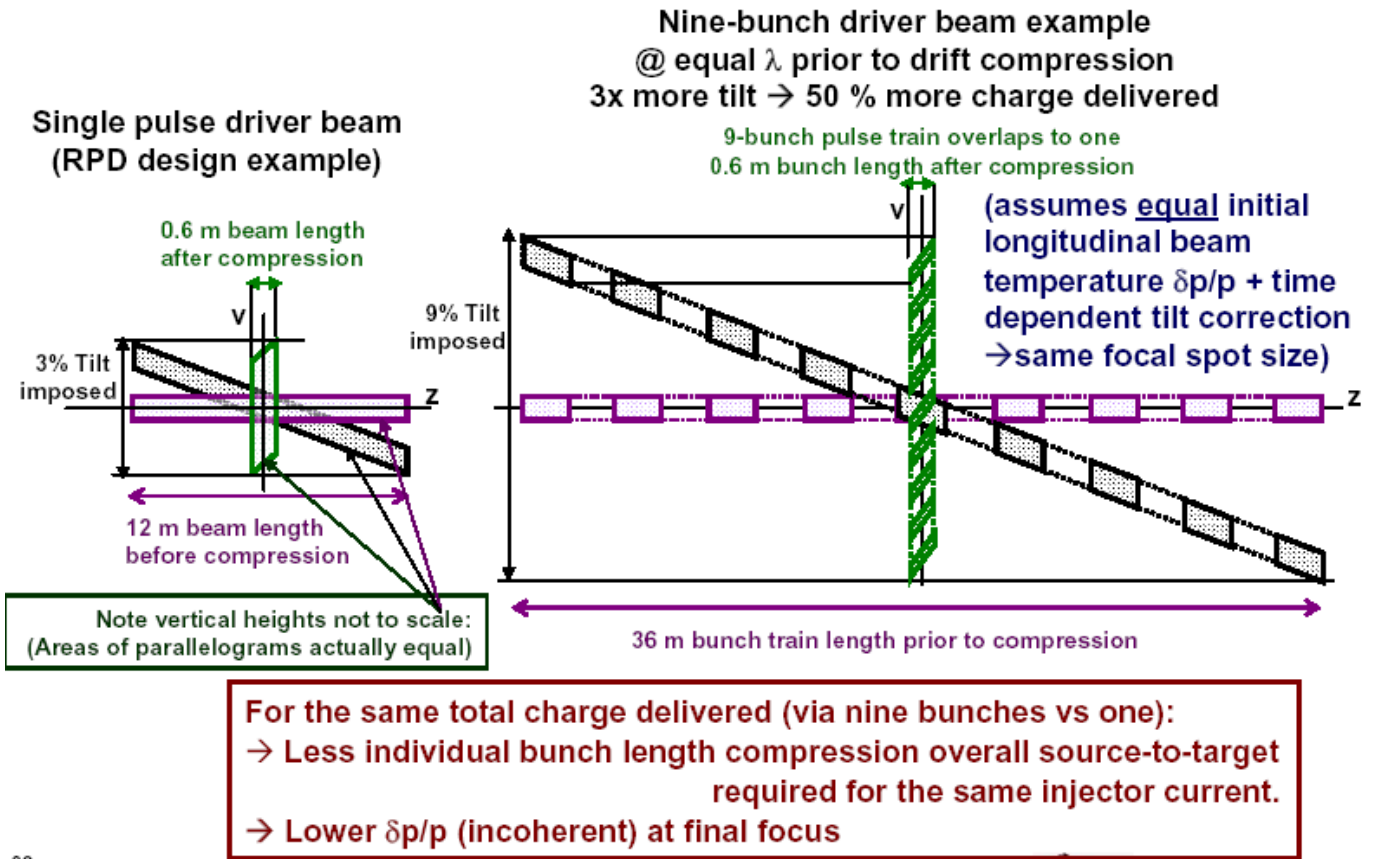


Figure 7 . Multi-pulse-train compression example ideally conserves longitudinal (v_z - z) phase space. *Time dependent focus allows larger tilt --> more beam intensity on target.*

(6) High gradient insulators that could become cheap in 30 years



(From George Caporaso's RPIA06 paper)

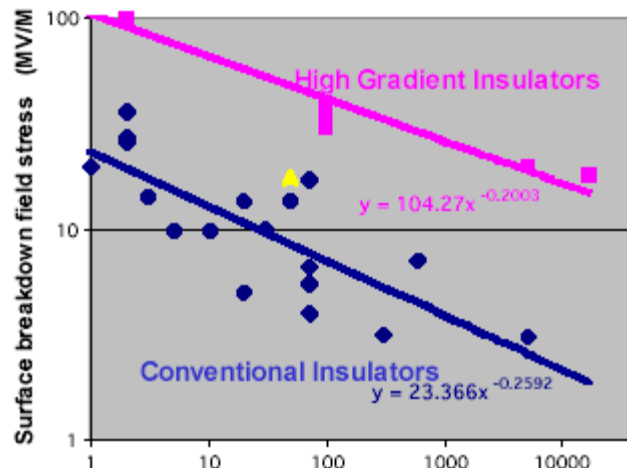


Figure 8. Closely-spaced conductors inhibit the breakdown process

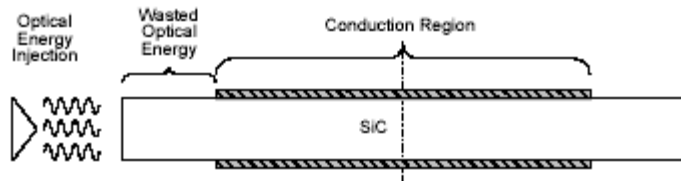
(7) Fast, compact (ultimately cheap) optically-gated solid state switches (Caporaso)



High Gradient Induction Cells Based on Advanced Insulators and Dielectrics*

G. J. Caporaso, S. Sampayan, M. Rhodes, Y.-J. Chen, J. Harris, B. Poole, L. Wang, J. Watson, J. Sullivan, D. Sanders
Lawrence Livermore National Laboratory

Workshop on Recent Progress in Induction Accelerators
KEK, Tsukuba, Japan
March 7-10, 2006



- **SiC photoconductive switch that closes AND opens promptly has been demonstrated at 27.5 MV/M gradient**

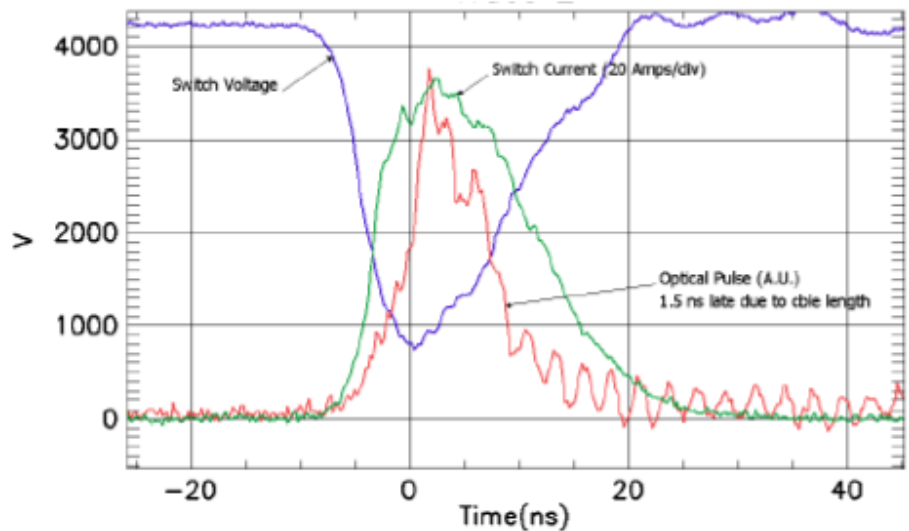
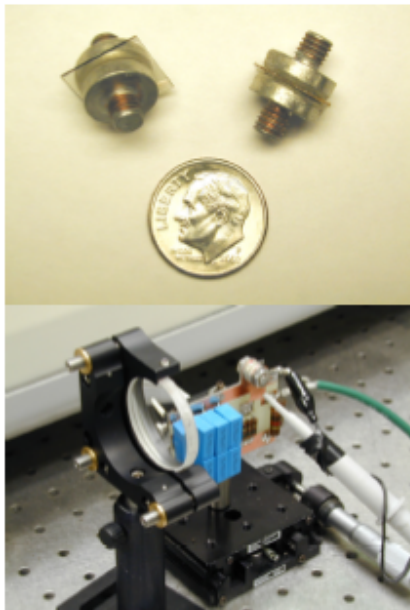


Figure 9. Proof-of-principle optically-driven SiC switch by LLNL Beam research team. WAG: 1 kA/cm² (Caporaso). Might scale to 30 cm² (hockey puck size) junction area ~ 30 kA, 30 kV-->1 GW per switch. If DPSSL-IFE diode laser cost used for gates-->negligible!

Assume 30 yr unit cost ~ \$1000/GW:

--> \$75 M for 75 TW switch power total for 25 TW beams x10X compression-->250TW target

$$UC_{pp} := 10^{-6}$$

\$/Watt, -->same as was assumed for thyratron pulse power in the RPD study!

(8) Low cost, low loss cores (Cheap Chinese cores in 30 years!)

$UC_{mc} := 5 \text{ \$/kg}$

2605C metglas $dB1 := 2.5$

$$Elc1(\tau_c) := 80.7 \cdot \left(\frac{dB1}{2.5}\right) + 193.3 \cdot \left(\frac{dB1}{2.5}\right) \cdot \sqrt{\frac{dB1}{\tau_c \cdot 10^6}} + 119.5 \cdot \left(\frac{dB1}{2.5}\right)^2 \cdot \frac{dB1}{\tau_c \cdot 10^6}$$

(Assumed for any of these four magnetic core materials in 30 yr)

CN-20 Ni-Zn Ferrite $dB2 := 0.38$

$$Elc2(\tau_c) := 240 \cdot \left(\frac{dB2}{2.5}\right) + 212.7 \cdot \left(\frac{dB2}{2.5}\right) \cdot \sqrt{\frac{dB2}{\tau_c \cdot 10^6}} + 3800 \cdot \left(\frac{dB2}{2.5}\right)^2 \cdot \frac{dB2}{\tau_c \cdot 10^6}$$

FT1H Finemet $dB3 := 2.0$

$$Elc3(\tau_c) := 50.7 \cdot \left(\frac{dB3}{2.5}\right) - 49.2 \cdot \left(\frac{dB3}{2.5}\right) \cdot \sqrt{\frac{dB3}{\tau_c \cdot 10^6}} + 200.4 \cdot \left(\frac{dB3}{2.5}\right)^2 \cdot \frac{dB3}{\tau_c \cdot 10^6}$$

TDK PE-11 ferrite $dB4 := 0.65$

(Special ferrite custom made for ETA/ATA)

$$Elc4(\tau_c) := 120 \cdot \left(\frac{dB4}{2.5}\right) + 50 \cdot \left(\frac{dB4}{2.5}\right) \cdot \sqrt{\frac{dB4}{\tau_c \cdot 10^6}} + 500 \cdot \left(\frac{dB4}{2.5}\right)^2 \cdot \frac{dB4}{\tau_c \cdot 10^6}$$

(LLNL report UCID-20786 April 21, 1986)

Plot from 30 μ s down to 20 ns

$$\tau_{cg} := 20 \cdot 10^{-9}, 40 \cdot 10^{-9} \dots 30 \cdot 10^{-6}$$

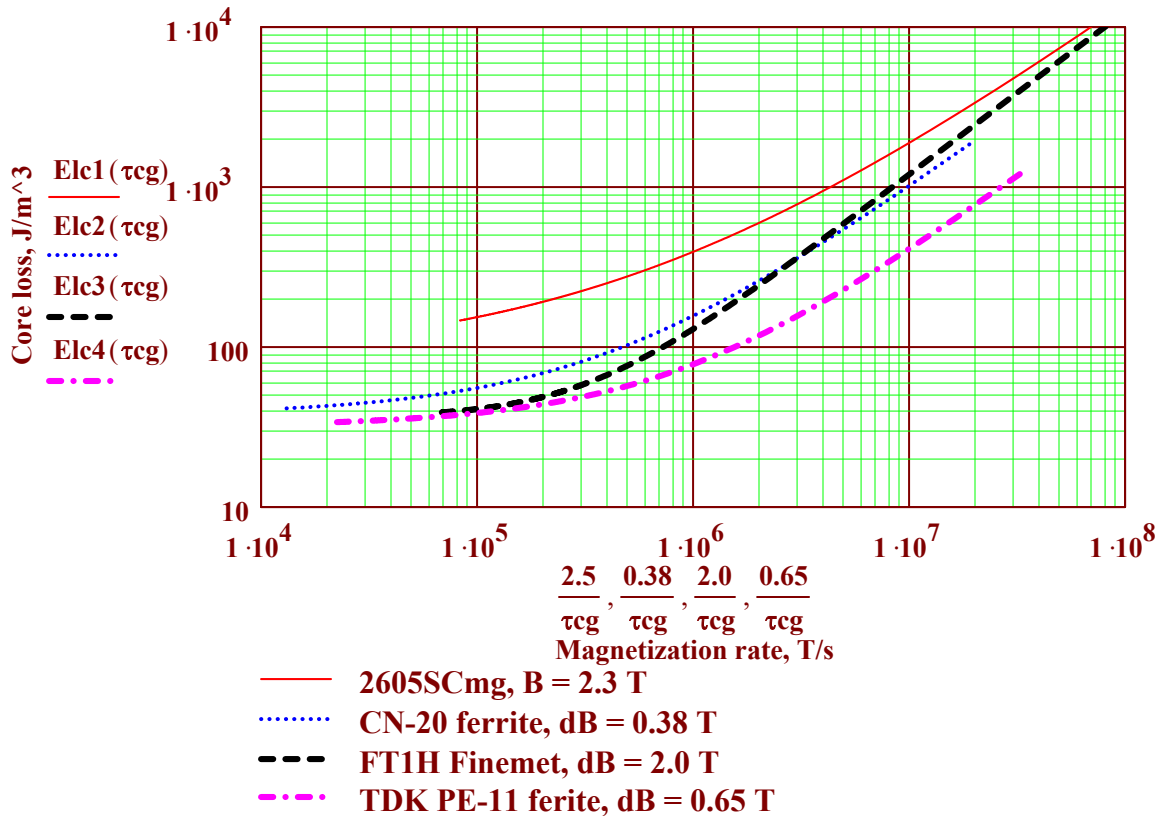
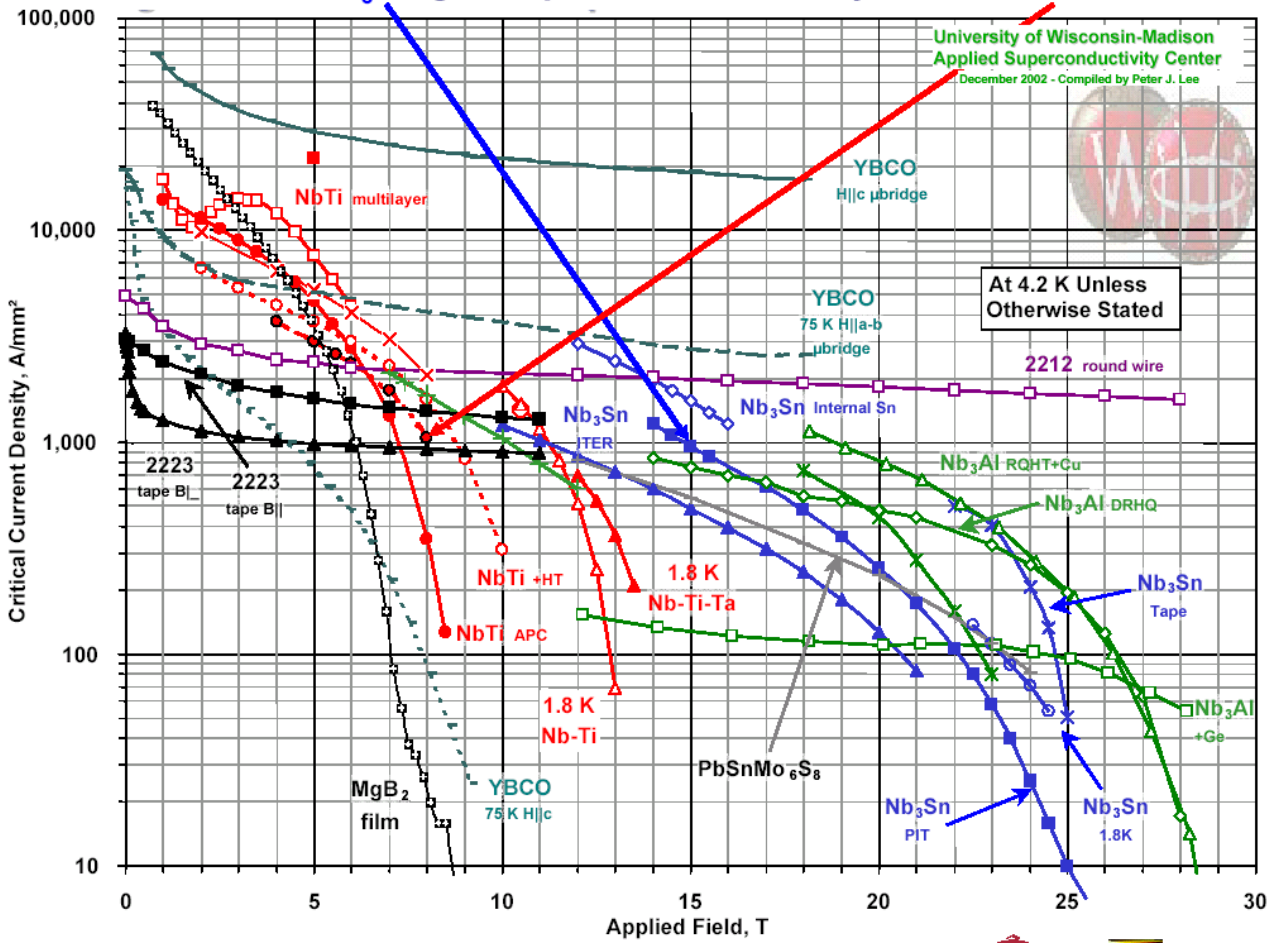


Figure 10. We assume the 30 yr price per kG of these candidates to be the same as the RPD assumption of \$5/kg. Gradient trades-offs with efficiency.

(9) Higher SC solenoid fields up to 15 T for the same price as NbTi in 30 years Figure 10

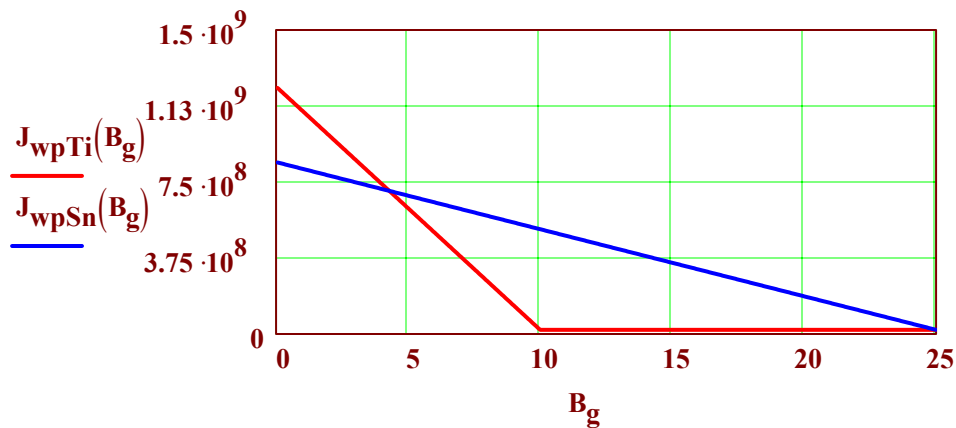
Advances in Nb₃Sn give equal current density at 15T as NbTi at 8 T



$J_0 := 1.2 \cdot 10^9$ Winding pack current density, A/m² @ zero field and 2.5 Cu:SC

$$J_{wpTi}(B) := J_0 \cdot \left(1 - \frac{B}{10}\right) \cdot \Phi\left(1 - \frac{B}{10}\right) + 2 \cdot 10^7 \quad J_{wpSn}(B) := \frac{J_0}{1.45} \cdot \left(1 - \frac{B}{25}\right) \cdot \Phi\left(1 - \frac{B}{25}\right) + 2 \cdot 10^7$$

$B_g := 0.05, 0.1.. 25$



$\mu_0 := 4 \cdot \pi \cdot 10^{-7}$

$J_{wpTi}(8) = 2.6 \times 10^8$

$J_{wpSn}(15) = 3.5 \times 10^8$

Winding thickness for 12 T solenoid

$$\frac{12}{\mu_0 \cdot J_{wpSn}(12)} = 0.021 \quad (m)$$

Figure 11 SC winding pack current density versus field, Nb₃Sn vs NbTi

(10) High power 500 kW 100 GHz ECR ion sources for high q ion injectors

Pulsed ECR source for high currents of high charge-state ions for HIF

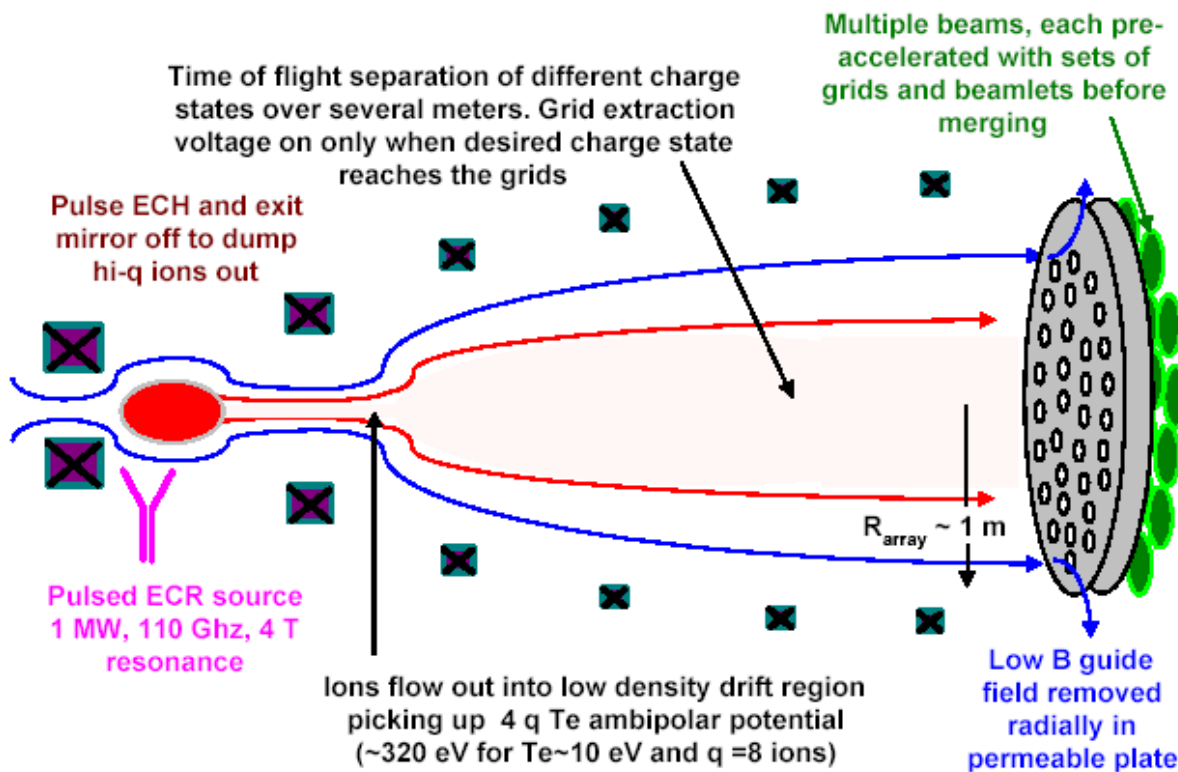


Figure 12. Conceptual hi-q ion ECR source from April 2002 notes with Daniella and Mattaheus Leitner and Joe Kwan, is similar to some Russian sources (see below). Below excerpts from proposal by Skalyga, Golubev (IAP-RAS) send to LBNL 2002:

"Quasi-Gasdynamic ECR source of plasma with multicharged ions (MCI).

Recent experimental and theoretical investigations carried out in IAP RAS allowed us to develop a new kind of pulsed ECR sources of MCI – quasi-gasdynamic ECR ion sources. On the base of these investigations we propose an ion source pumped by 100 GHz, 500 kW gyrotron with 1 ms pulse duration. Such a quasi-gasdynamic ECR source is able to generate pulsed plasma flows with maximum of the ion charge state distribution and ion current density as shown in Table 1. Typical transversal dimension of plasma flow is 1 cm."

Gas dynamic ECR plasma source	Plasma ion separator	Ion extractor
-------------------------------	----------------------	---------------

Carbon	+4	14 A/cm ²
Nitrogen	+5	14 A/cm ²
Oxygen	+6	14 A/cm ²
Argon	+8	11 A/cm ²
Xenon	+14	7 A/cm ²

These Russian capabilities should be a good match for the ModSoLinac Multi-pulse example shown above in Fig. 1

A quick first look example of how these innovations might apply:

Constants, basic quantities

$c := 3 \cdot 10^8$ (m/s) the speed of light,

$\epsilon_0 := 8.85 \cdot 10^{-12}$ Vacuum permittivity (Farads/m),

$\mu_0 := 4 \cdot \pi \cdot 10^{-7}$ Vacuum permeability (Henrys/m)

$m_e := 9.1 \cdot 10^{-31}$ (kg), electron mass $e := 1.6 \cdot 10^{-19}$ (Coulomb) Electron charge

$M_p := 1.67 \cdot 10^{-27}$ (kg) Proton Mass $I_0 := 3.1 \cdot 10^7$ (Amps) -constant in beam perveance

The relativistic gamma and beta, with T the kinetic energy in eV, A the atomic mass number

$$\gamma(T, A) := 1 + \frac{e \cdot T}{A \cdot M_p \cdot c^2}$$

$$\beta(T, A) := \sqrt{1 - \gamma(T, A)^{-2}}$$

$$\beta\gamma(T, A) := \beta(T, A) \cdot \gamma(T, A)$$

Independent variables we specify:

The total beam energy, W_b onto the target, with nominal value $W_{b0} := 1 \cdot 10^6$ J

The number of modular linacs / beams N_b , with nominal value $N_{b0} := 40$

The number of pulses per linac per shot N_p , with nominal value $N_{p0} := 5$

The chosen ion mass A, with nominal value $A_0 := 40$

The chosen ion charge state q, with nominal value $q_0 := 8$

The final tail ion kinetic energy T_f for nominal range 0.04 g/cm² $T_{f0} := 6 \cdot 10^8$ eV

The final head bunch ion kinetic energy (for 10 % $\Delta v/v$) $T_{fho} := T_{f0} \cdot 1.2^{-1}$

The nominal single ion bunch full length $L_{b0} := 2$ (m)

Most beam quantities will be calculated along the accelerator as functions of the local ion energy T or voltage V, with optimizations to determine the local bunch length L_b and solenoid magnetic field B_s which minimize cost.

The charge per bunch is $Q(q, T_f, W_b, N_b, N_p) := \frac{q \cdot 1.1 \cdot W_b}{T_f \cdot N_b \cdot N_p}$ Eq. 1

Nominal $Q(q_0, T_{f0}, W_{b0}, N_{b0}, N_{p0}) = 7.33 \times 10^{-5}$ (C)

Integrated induction acceleration with longitudinal bunch confinement and core reset

Triangular or cos²-shaped line-charge-density profiles most naturally arise and are similar to what Dave Grote simulated for the NDCX experiment. They are perfectly acceptable for target pulse shapes to be constructed by a "picket fence" of many pulses, and also, such line charge profiles moderate ears and the amount of forced waveform shaping required using agile waveform modulation.

Longitudinal bunch confinement is necessary during acceleration and requires time-averaged applied "ear fields" equal to the self-field $E_{bz} \sim \lambda_0 / (2\pi\epsilon_0 L_b)$ where the bunch (full) length = L_b . Lets consider a \cos^2 profile for $\lambda(z)$, plotted in the Figure below.

$$\lambda_b(q, T_f, W_b, N_b, N_p, L_b, z) := \frac{2 \cdot Q(q, T_f, W_b, N_b, N_p)}{L_b} \cdot \cos\left(\frac{\pi}{L_b} \cdot z\right)^2 \cdot \Phi\left(1 - \frac{2 \cdot z}{L_b}\right) \quad \text{C/m Eq. 2}$$

$$E_{bz}(q, T_f, W_b, N_b, N_p, L_b, z) := \frac{-Q(q, T_f, W_b, N_b, N_p)}{2 \cdot \epsilon_0 \cdot L_b^2} \cdot \sin\left(\frac{2 \cdot \pi}{L_b} \cdot z\right) \cdot \Phi\left(1 - \frac{2 \cdot z}{L_b}\right) \quad \text{V/m Eq. 3}$$

Integrated induction field E_n waveforms must provide constant net average acceleration field E_a across the bunch as well as reset of the cores. Reset times ~ acceleration pulse times will keep peak reset voltages ~ peak acceleration voltages.

$$E_n(q, T_f, W_b, N_b, N_p, L_b, z, E_a) := E_a + E_{bz}(q, T_f, W_b, N_b, N_p, L_b, z) \dots \quad \text{V/m Eq. 4}$$

$$+ -3 \cdot E_a \cdot \cos\left[\frac{\pi}{2 \cdot L_b} \cdot \left(z + \frac{L_b}{2}\right)\right]^2 \cdot \Phi\left(\frac{2 \cdot z}{L_b} - 1\right)$$

For a nominal acceleration gradient

$$E_{ao} := 1.5 \cdot 10^6 \quad \text{V/m} \quad z_p := \left(-L_{bo} \cdot 2^{-1}\right), \left(-L_{bo} + 0.01\right) \cdot 2^{-1} \dots 2.5 \cdot L_{bo}$$

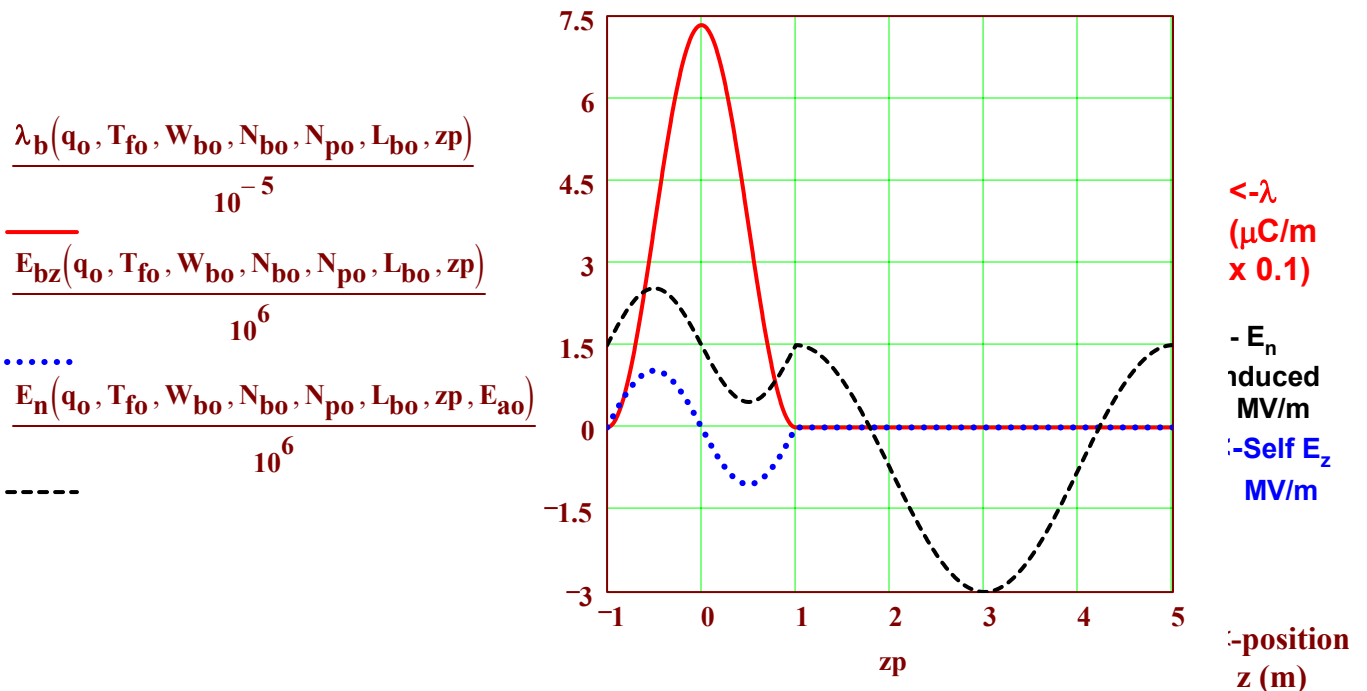


Figure 13. Example induction waveform integrating acceleration, "ears", and reset. Note the useful full bunch length (duration) in this example is one-third of the total core cycle time, while the effective accelerating induction pulse duration is one-half of the total core cycle time. This example shows that the chosen charge/bunch length is near maximum, keeping $E_{bz} < E_{ao}$.

Peak line charge density $\lambda_p(q, T_f, W_b, N_b, N_p, L_b) := 2 \cdot \frac{Q(q, T_f, W_b, N_b, N_p)}{L_b}$ (C/m) Eq. 5

For our example, during injection into the pre-bunch section (see Fig. 1), the bunch length is 12 m (3X shorter than for the RPD design single bunch length at injection)

$$\lambda_p(q_0, T_{fo}, W_{bo}, N_{bo}, N_{po}, 12) = 1.22 \times 10^{-5} \quad (\text{C/m})$$

After pre-bunching by a factor 6 x down to 2 meter bunches throughout the rest of the linac:

$$\lambda_p(q_0, T_{fo}, W_{bo}, N_{bo}, N_{po}, L_{bo}) = 7.3 \times 10^{-5} \quad (\text{C/m})$$

The effective core ramp time τ_c (acceleration pulse) shown in the above Fig 12 is 1.5X longer than the bunch temporal pulse duration due to bunch length control and reset, and depends on the ion

local velocity/energy/voltage V : $\tau_c(q, V, A, L_b) := \frac{1.5 \cdot L_b}{\beta(q \cdot V, A) \cdot c}$ (s). Eq. 6

At injection and fire times [Argon 8+ @100 kV net (accel-decel) =800 keV at $q = 8$], core pulses

$$\tau_c(q_0, 10^5, A_0, 6 \cdot L_{bo}) = 9.2 \times 10^{-6} \quad \& \quad \tau_c(q_0, 10^5, A_0, L_{bo}) = 1.5 \times 10^{-6} \quad \text{s, respectively.}$$

At the final linac energy (tail bunch) $T_{fo} = 6 \times 10^8$ (eV), or $T_{fo} \cdot q_0^{-1} = 7.5 \times 10^7$ Volts

the core accel-pulse time is $\tau_c(q_0, T_{fo} \cdot q_0^{-1}, A_0, L_{bo}) = 5.7 \times 10^{-8}$ (s)

Injecting (loading) a 5-pulse train [five 12-m bunches with four 2-m reset lengths (1 μ s reset times) in between bunches] takes a total length $(5 \cdot 6 + 4) \cdot L_{bo} = 68$ m and total time

$$(5 \cdot 6 + 4) \cdot L_{bo} \cdot \left(\beta(q_0 \cdot 1 \cdot 10^5, A_0) \cdot c \right)^{-1} = 3.5 \times 10^{-5} \quad \text{s}$$

Pre-bunching 12m injected bunches into trains of 2m-long bunches before acceleration.

By repetitively ramping down (reducing) the 300 kV *decel* voltage during injection (Enrique's suggestion), each 12 m bunch can be given an initial 15 -30 % $\Delta v/v$ tilt going into the pre-bunch section, enough to compress each bunch to the desired L_{bo} lengths by the time each bunch reaches its desired position for load and fire. In most cases the self space charge can be arranged to stagnate (remove) much of the bunch compression tilt. Variable but modest ~100-200 kV/m average ear pulses in the pre-bunch section can fine-tune the process of loading-in constant energy and spacings of bunches to achieve the load and fire pulse train length

$$L_{lf} := \left[N_{po} + 2 \cdot (N_{po} - 1) \right] \cdot L_{bo} \quad L_{lf} = 26 \quad \text{m.}$$

Minimizing the total required pre-bunch length L_{bp} + load and fire section length L_{lf} together will usual require a total length $\sim 3 L_{lf}$, or a pre-bunch length $\sim 2 L_{lf}$. Details on this later.

$$3 \cdot L_{lf} = 78 \quad \text{m} \quad L_{pb} := 2 \cdot L_{lf} \quad L_{pb} = 52 \quad \text{m.}$$

High q ion source and injector parameters

The required source current of Ar^{+8} during each bunch injection is

$$I_s := 1.5 \cdot Q(q_0, T_{f0}, W_{b0}, N_{b0}, N_{p0}) \cdot \tau_c(q_0, 1 \cdot 10^5, A_0, 6 \cdot L_{b0})^{-1} \quad I_s = 12 \quad \text{A} \quad \text{Eq. 7}$$

Equivalent to 4 A K^+ . Matches Russian Ar^{+8} ECR source (Fig.11)

Assuming 100 kV/cm in the first 1 cm extraction gap and beyond, an average beamlet extraction occupancy factor of 0.2, the extractable plasma source array average current density

$$J_{\text{CL}}(q, A) := \frac{0.2 \cdot (5.46 \cdot 10^{-8})}{0.01^2} \cdot \sqrt{\frac{q \cdot (100 \cdot 10^3)^3}{A}} \quad J_{\text{CL}}(q_0, A_0) = 1544 \quad \text{A/m}^2 \quad \text{Eq 8}$$

The required multi-beamlet source array size for a large single beams:

$$a_s(I_s, q, A) := \sqrt{\frac{I_s}{\pi \cdot J_{\text{CL}}(q, A)}} \quad a_s(I_s, q_0, A_0) = 0.05 \quad (\text{m}) \quad \text{Eq. 9}$$

Ar^{+8} plasma source diameter ~ current 4 " hot plates

The injection bunch frequency (within a 5-pulse burst) is:

$$\left(\tau_c(q_0, 1 \cdot 10^5, A_0, 6 \cdot L_{b0}) \cdot 1.5^{-1} + 1 \cdot 10^{-6} \right)^{-1} = 1.4 \times 10^5 \quad \text{Hz}$$

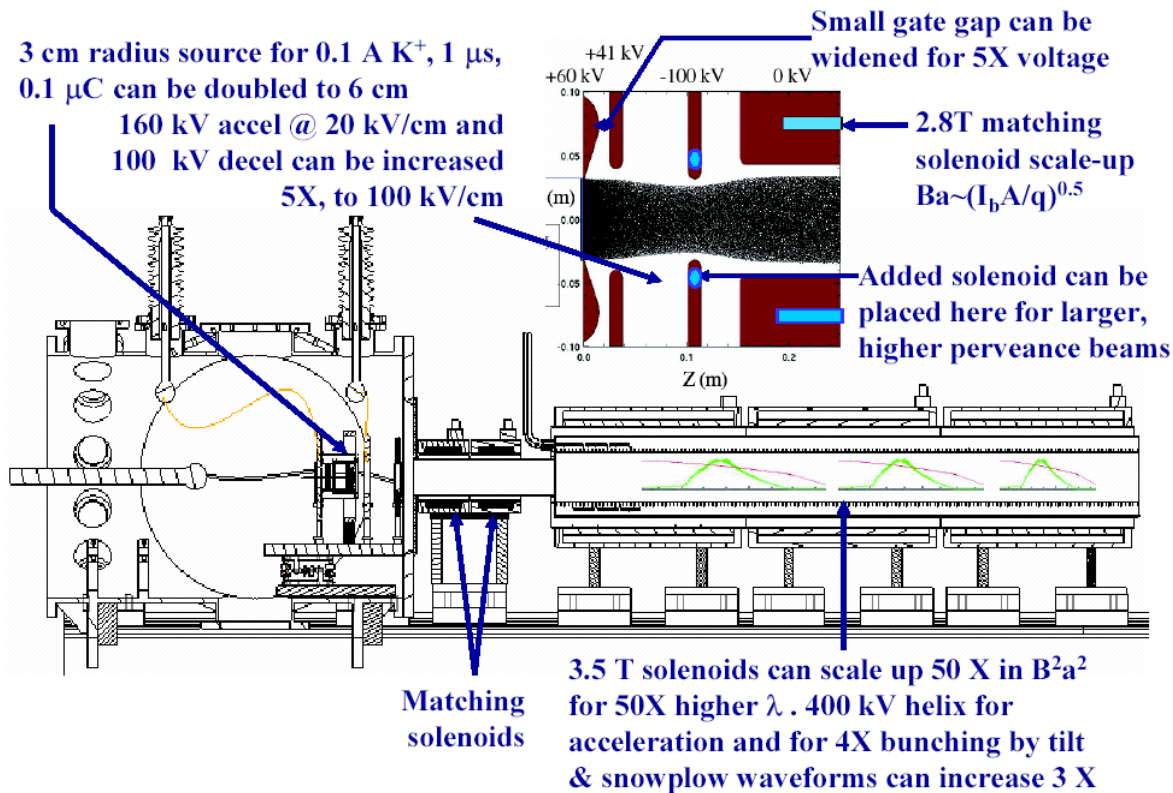


Fig. 14. Illustration of how an accel-decel injector design by Enrique for NDCX-II can be scaled up for a PLIA-IFE driver. These enhancements can also apply to induction drivers.

Acceleration and linac length

The required total core volt-seconds per meter for a repeating waveform of the above shape and for given acceleration gradient E_a can be expressed as:

$$\Delta B_c dR_c PF_r PF_z = E_a \tau_c$$

where ΔB_c is the core flux swing, dR_c is the core radial build, PF_r and PF_z are the radial and axial effective core packing fractions, respectively. Since the bunch/core pulse duration τ_c varies by a large factor with voltage V from the injection end of the linac to the high energy end, either the core radial build dR_c or the average local gradient E_a , or both, have to vary along the linac. To maximize commonality of part dimensions for lower mass production costs, we prefer to keep the core radial build constant along the linac, and solve for the resultant allowed gradients as a function of voltage along the linac. Let's first take finemet as the core material for our example:

$dB3 = 2$ (T) and assume $PF_r := 0.8$ $PF_z := 0.6$ radial and axial packing fractions.

The resulting local acceleration gradient as a function of ion energy (voltage) is

$$E_{ao}(q, V, A, L_b, dR_c) := \frac{dB3 \cdot dR_c \cdot PF_r \cdot PF_z}{\tau_c(q, V, A, L_b)} \quad \text{V/m} \quad \text{Eq. 10}$$

Assuming a **modest, constant core radial build** $dR_{c0} := 0.15$ (m)

Fig. 14 plots the resulting local gradient E_a , the local core accel time τ_c , $V_z := 10^5, 2 \cdot 10^5 \dots \frac{T_{fho}}{q_0}$ and distance L_a to voltage V as functions of the voltage V along the linac

$$L_a(q, V, A, L_b, dR_c) := \int_{10^5}^V E_{ao}(q, V, A, L_b, dR_c)^{-1} dV \quad \text{(m)} \quad \text{Eq. 11}$$

from injection energy = $q \times 100\text{kV} = 800$ eV up to the final head energy $T_{fho} \cdot q_0^{-1} = 6.25 \times 10^7$

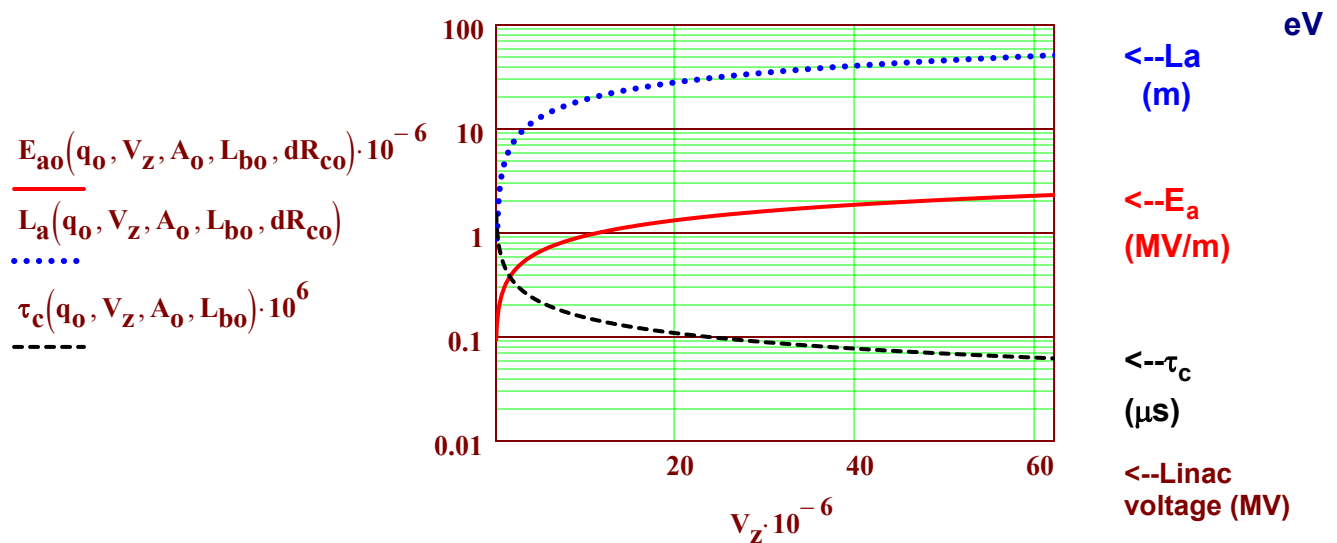


Figure 15. Local acceleration gradient, acceleration distance (injection to voltage V), and local core accel times as a function of voltage along the linac up to the head pulse energy.

$L_{b0} = 2$ m $N_{p0} = 5$ pulses

Core $dR_{c0} = 0.15$ m, finemet

5-bunch train acceleration

In the example shown in (Fig.1) the accelerating section has to accelerate five bunches using a common set of cores, the first bunch to the head energy, and the last to the tail energy 20 % higher to provide 10% tilt for NDC, and the in-between bunches to energies in between. The required acceleration distances for each bunch, using the same set of cores with constant volt-seconds per meter (constant dR_c) and with constant and equal bunch lengths L_{b0} are :

$$\begin{aligned}
 \text{La1} &:= \text{ceil} \left[L_a \left(q_0, \frac{T_{fho}}{q_0}, A_0, L_{b0}, dR_{c0} \right) \right] & \text{La1} &= 52 & \text{m, Head pulse} \\
 \text{La2} &:= \text{ceil} \left[L_a \left(q_0, \frac{(T_{fo} + 3 \cdot T_{fho})}{4 \cdot q_0}, A_0, L_{b0}, dR_{c0} \right) \right] & \text{La2} &= 53 & \text{m} \\
 \text{La3} &:= \text{ceil} \left[L_a \left(q_0, \frac{(T_{fo} + T_{fho})}{2 \cdot q_0}, A_0, L_{b0}, dR_{c0} \right) \right] & \text{La3} &= 54 & \text{m} \\
 \text{La4} &:= \text{ceil} \left[L_a \left(q_0, \frac{(3 \cdot T_{fo} + T_{fho})}{4 \cdot q_0}, A_0, L_{b0}, dR_{c0} \right) \right] & \text{La4} &= 56 & \text{m} \\
 \text{La5} &:= \text{ceil} \left[L_a \left(q_0, \frac{T_{fo}}{q_0}, A_0, L_{b0}, dR_{c0} \right) \right] & \text{La5} &= 57 & \text{m, Tail pulse}
 \end{aligned}$$

Here we have rounded off the lengths to the nearest higher integer to aid pulse-train analysis with discrete 1-meter core acceleration blocks below, accepting a small innacuracy in the rounding-off.

We can solve for the voltages attained for given distances of acceleration La under the constant core radial build and constant bunch length (constant λ) assumptions, starting at an initial bunch energy/voltage V_0 : Initial guess $V := 10^5$

$$V_a(q, La, V_0, A, L_b, dR_c) := \text{root} \left[\left[\int_{V_0}^V E_{a0}(q, V, A, L_b, dR_c)^{-1} dV - La \right], V \right] \quad \text{Volts, Eq. 12}$$

Check $V_a(q_0, 51.3, 10^5, A_0, L_{b0}, dR_{c0}) = 6.26 \times 10^7 \quad V$

Now lets plot the trajectories of the five bunches along distance:

with mid-bunch starting positions m, and starting voltages $V_0 := 10^5 \quad V$,

and for $i1 := 1..La1$ 1-meter-long induction modules centered at positions $z1_{i1} := 23.5 + i1$
 $i2 := 1..La2$ $z2_{i2} := 17.5 + i2$
 $i3 := 1..La3$ $z3_{i3} := 11.5 + i3$
 $i4 := 1..La4$ $z4_{i4} := 5.5 + i4$
 $i5 := 1..La5$ $z5_{i5} := -0.5 + i5$

The corresponding bunch voltage array versus distance (remember to multiply voltages by charge q_0 to get bunch energies) at each cell block mid-plane in 1 meter intervals) :

$V_{a1i1} := V_a(q_0, z_{1i1} - 24, V_0, A_0, L_{b0}, dR_{c0})$	$V_{a1La1} = 6.306 \times 10^7$	(The last element in each bunch array is the final desired voltage for each bunch, when rounding off to the nearest cell block)
$V_{a2i2} := V_a(q_0, z_{2i2} - 18, V_0, A_0, L_{b0}, dR_{c0})$	$V_{a2La2} = 6.542 \times 10^7$	
$V_{a3i3} := V_a(q_0, z_{3i3} - 12, V_0, A_0, L_{b0}, dR_{c0})$	$V_{a3La3} = 6.782 \times 10^7$	
$V_{a4i4} := V_a(q_0, z_{4i4} - 6, V_0, A_0, L_{b0}, dR_{c0})$	$V_{a4La4} = 7.275 \times 10^7$	
$V_{a5i5} := V_a(q_0, z_{5i5}, V_0, A_0, L_{b0}, dR_{c0})$	$V_{a5La5} = 7.527 \times 10^7$	

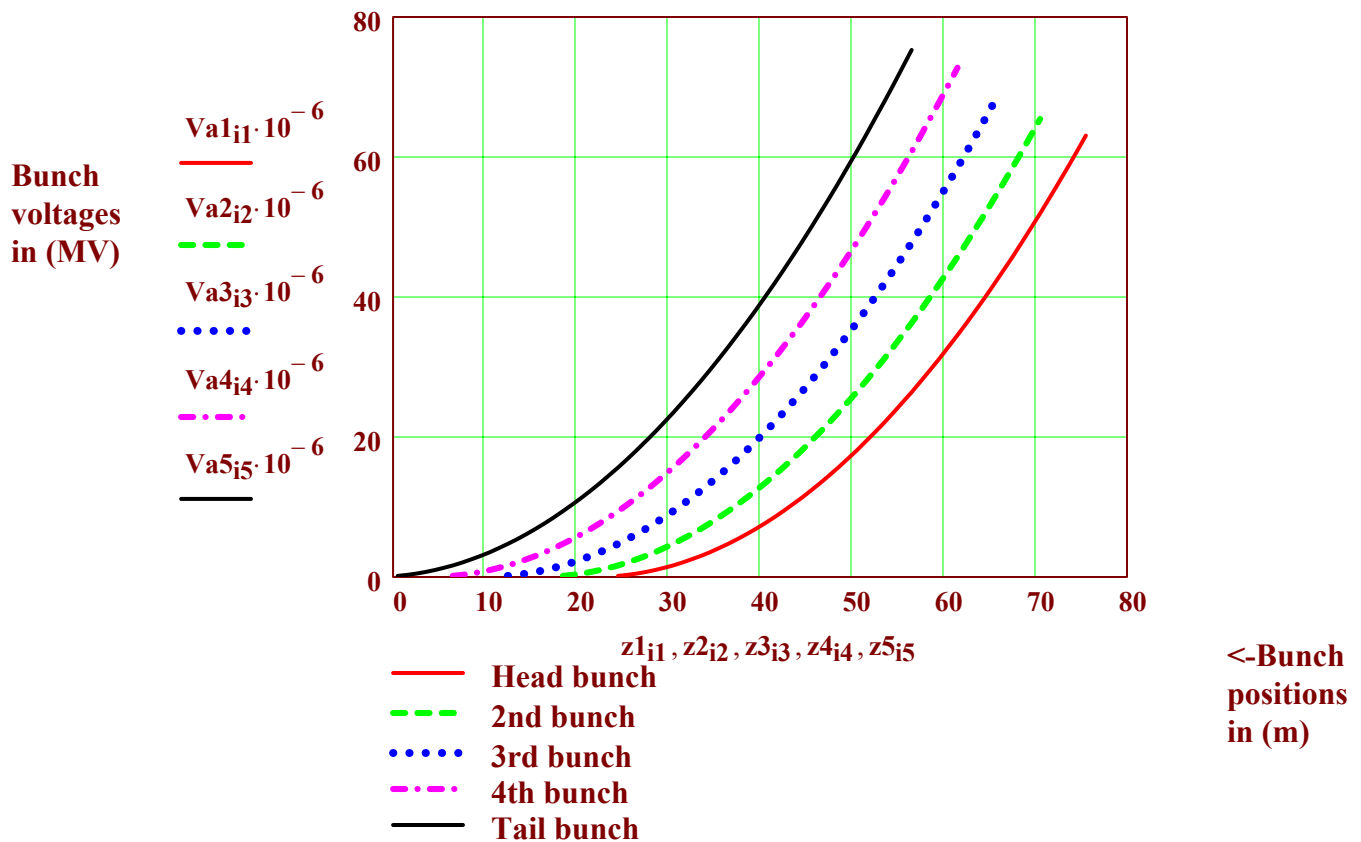


Figure 16. Bunch voltages (MV) versus positions (m) for 5-bunch pulse train acceleration under constant volt seconds per meter ($dR_c=15$ cm finemet cores), and constant bunch lengths ($L_{b0}=2$ meters).

Note in Fig. 15 that the bunches maintain constant spacings of 6 meters between bunch centers during the chosen load-and-fire acceleration schedule. Using a common set of cores, a total length of $z_{1La1} = 76$ meters of accelerator is needed total, with different bunches requiring different portions of the set of cores to fire at different times. The first core at $z = 0$ fires only one cycle to start the tail bunch, the last core also only fires one cycle to finish the head bunch; most cores in-between fire five cycles. The bunches come out with the desired 20 % energy spread for 10% velocity tilt for NDC.

Radial bunch confinement: acceleration module radial build for solenoid transport.

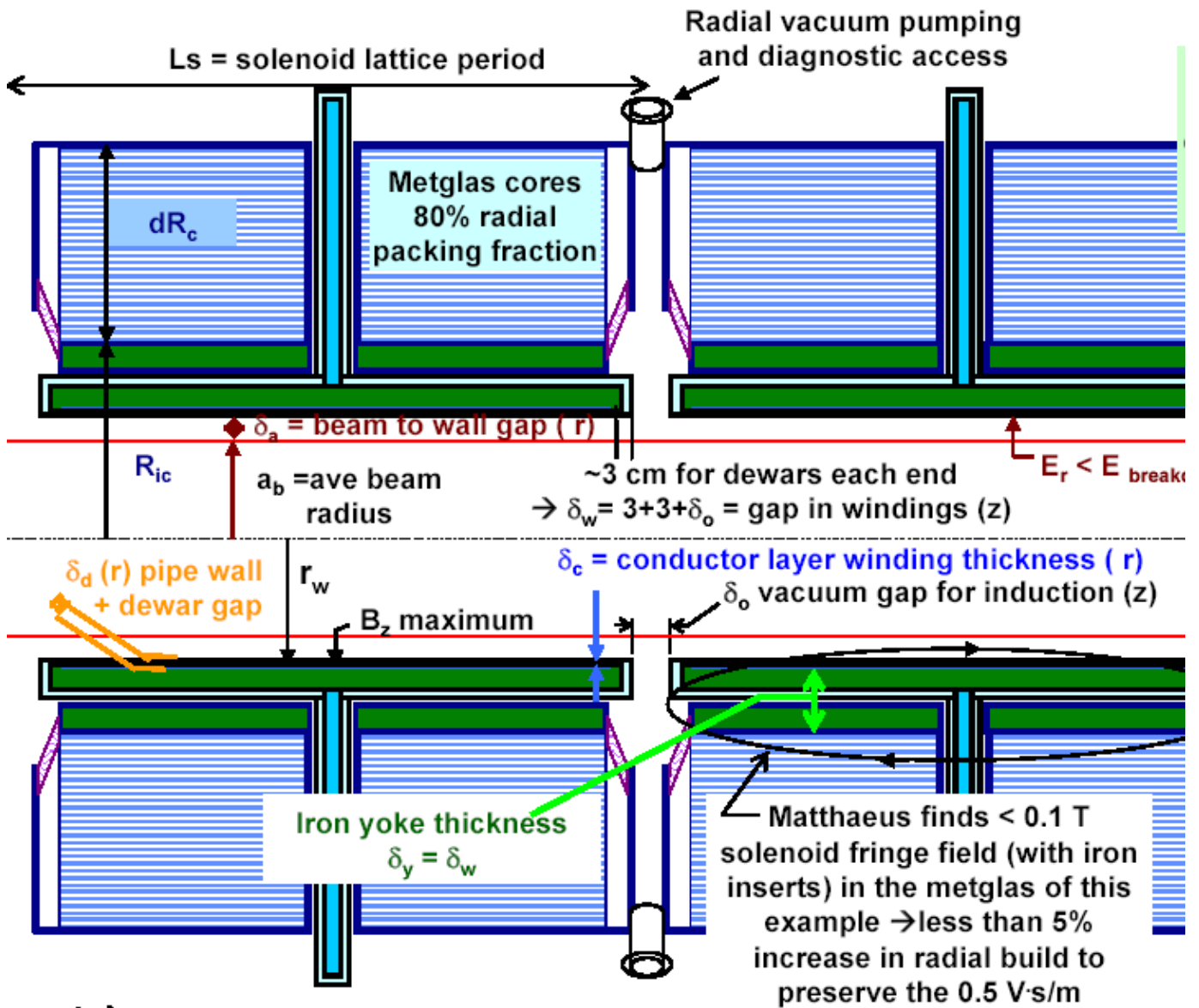


Figure 17 The solenoid linac section with elements identified in the radial build for cost model (from June 11, 2003 talk). At >1-2 MV/m, there may be 4, 6 or 8 cores per magnet, especially to ameliorate discrete acceleration effects on short bunches.

A nice property of solenoid transport is the required beam radius a_b and solenoid field B_s is a function only of the line-charge density, independent of the ion velocity. For a constant bunch length in the accelerator sections (see Fig. 16), the bunch line charge density is constant, and so the current scales with ion velocity (voltage) along the linac (Figure 17 next).

$$I_b(q, A, T_f, V, W_b, N_b, N_p, L_b) := \lambda_p(q, T_f, W_b, N_b, N_p, L_b) \cdot \beta(q \cdot V, A) \cdot c(A) \quad \text{Eq. 13}$$

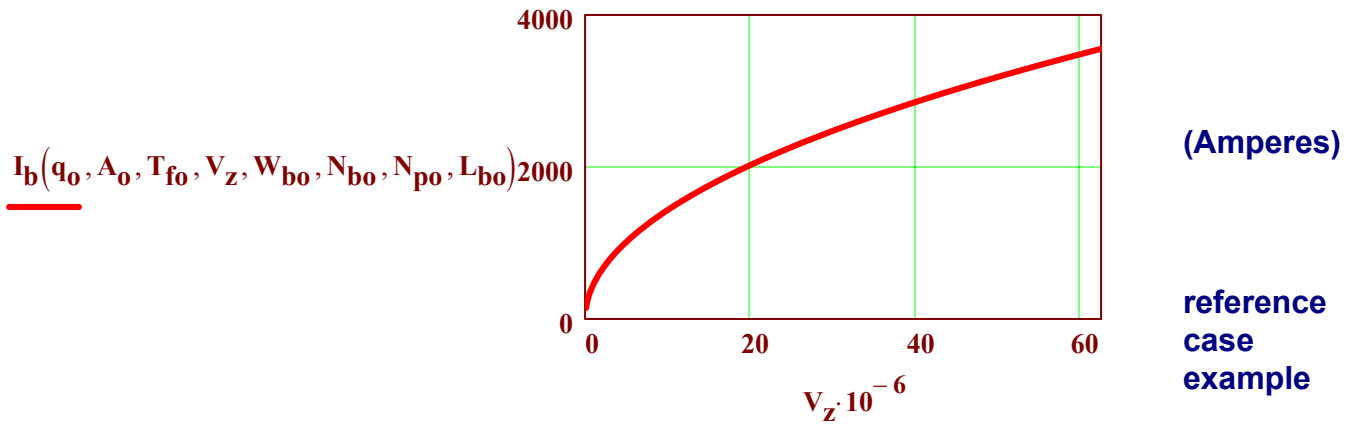


Figure 18. Single beam peak current of Ar⁸⁺ as a function of voltage along the linac

From the transportable current formula for a solenoid

$$\lambda_p = I_b / \beta \gamma c = 4 \cdot 10^5 (q/A) B_s^2 a_b^2 \eta_s / c \quad \text{Eq. 14}$$

where η_s is the effective B_s^2 average solenoid field occupancy, we can solve for the beam radius a_b :

$$a_b(q, A, T_f, W_b, N_b, N_p, L_b, B_s, \eta_s) := \sqrt{\frac{\lambda_p(q, T_f, W_b, N_b, N_p, L_b) \cdot c}{4 \cdot 10^5 \cdot \left(\frac{q}{A}\right) \cdot B_s^2 \cdot \eta_s}} \quad \text{(m)} \quad \text{Eq. 15}$$

Desirably, to keep the acceleration module dimensions uniform, we would like to keep the beam radius as well as the pipe wall and core radial build dR_c all constant with z or with beam energy along with the constant beam line charge density. Later on we will show that the effective solenoid occupancy factor must slowly decrease with higher local acceleration gradients due to the need for larger induction gaps with higher gradients (for voltage holding). We defer these details for now, but use the effective occupancy factor for 1.5 MV/m:

This gives a reference case (nearly constant) beam radius:

$$\eta_{s0} := 0.75 \quad B_{s0} := 12$$

$$a_b(q_0, A_0, T_{f0}, W_{b0}, N_{b0}, N_{p0}, L_{b0}, B_{s0}, \eta_{s0}) = 0.05 \quad \text{(m)}$$

...at the field = 12 T (to be optimized)

-->~ twice the maximum size beam radius in the current NDCX experiment using 3 T solenoids.

For a 80% beam fill factor, the pipe wall radius

$$r_p(q, A, T_f, W_b, N_b, N_p, L_b, B_s, \eta_s) := a_b(q, A, T_f, W_b, N_b, N_p, L_b, B_s, \eta_s) \cdot 0.8^{-1}$$

$$r_p(q_0, A_0, T_{f0}, W_{b0}, N_{b0}, N_{p0}, L_{b0}, B_{s0}, \eta_{s0}) = 0.063 \quad \text{m.} \quad \text{Eq. 16}$$

Adding 2 cm for the dewar, the inner coil winding radius

$$r_{wi}(q, A, T_f, W_b, N_b, N_p, L_b, B_s, \eta_s) := r_p(q, A, T_f, W_b, N_b, N_p, L_b, B_s, \eta_s) + 0.02 \text{ m. Eq. 17}$$

$$r_{wi}(q_0, A_0, T_{fo}, W_{bo}, N_{bo}, N_{po}, L_{bo}, B_{so}, \eta_{so}) = 0.083 \text{ m.}$$

The outer sc winding radius r_{wo} is larger by the required winding pack thickness:

$$r_{wo}(q, A, T_f, W_b, N_b, N_p, L_b, B_s, \eta_s) := r_{wi}(q, A, T_f, W_b, N_b, N_p, L_b, B_s, \eta_s) + \frac{B_s}{\mu_0 \cdot J_{wpSn}(B_s)}$$

$$r_{wo}(q_0, A_0, T_{fo}, W_{bo}, N_{bo}, N_{po}, L_{bo}, B_{so}, \eta_{so}) = 0.104 \text{ m. Eq. 18}$$

A 4 cm cryogenic manganese iron yoke for magnetic load support and core shielding, plus 2 cm for the outer cold dewar thickness, and 1 cm for a room temperature core housing inner pipe wall and insulation, brings us to the the inner core radius (see Fig.16):

$$R_{ic}(q, A, T_f, W_b, N_b, N_p, L_b, B_s, \eta_s) := r_{wo}(q, A, T_f, W_b, N_b, N_p, L_b, B_s, \eta_s) + 0.07 \text{ m. Eq.19}$$

$$R_{ic}(q_0, A_0, T_{fo}, W_{bo}, N_{bo}, N_{po}, L_{bo}, B_{so}, \eta_{so}) = 0.17 \text{ m.}$$

The outer core radius for our reference example, with $dR_{co} = 0.15 \text{ m}$, is then

$$R_{ic}(q_0, A_0, T_{fo}, W_{bo}, N_{bo}, N_{po}, L_{bo}, B_{so}, \eta_{so}) + dR_{co} = 0.324 \text{ m.}$$

The total core mass for the small driver system can be estimated now, neglecting the few cores needed for ear control in the prebunch drift section to get a quick look. For

$N_{bo} = 40$ linacs and for $\rho_{mc} := 7000 \text{ kg/m}^3$ mass density (finemet or metglas)

$$M_{mc}(q, A, T_f, W_b, N_b, N_p, L_b, L_a, B_s, \eta_s, dR_c) := \frac{2 \cdot R_{ic}(q, A, T_f, W_b, N_b, N_p, L_b, B_s, \eta_s) \cdot dR_c + dR_c^2}{(\rho_{mc} \cdot N_b \cdot \pi \cdot L_a \cdot PF_r \cdot PF_z)^{-1}}$$

$$M_{mc}(q_0, A_0, T_{fo}, W_{bo}, N_{bo}, N_{po}, L_{bo}, z1La1, B_{so}, \eta_{so}, dR_{co}) = 2.4 \times 10^6 \text{ kg. Eq. 20}$$

At RPD unit costs $UC_{mc} = 5 \text{ \$/kg}$, the total direct cost of magnetic core material is

$$C_{mc}(q, A, T_f, W_b, N_b, N_p, L_b, L_a, B_s, \eta_s, dR_c) := \frac{M_{mc}(q, A, T_f, W_b, N_b, N_p, L_b, L_a, B_s, \eta_s, dR_c)}{UC_{mc}^{-1}}$$

$$C_{mc}(q_0, A_0, T_{fo}, W_{bo}, N_{bo}, N_{po}, L_{bo}, z1La1, B_{so}, \eta_{so}, dR_{co}) = 1.2 \times 10^7 \text{ \$ Eq. 21}$$

The 2003 modular solenoid driver study with 16 linacs had 7000 tons of metglas for 6.4 MJ. This new multi-pulse example has roughly 7.5 X less total core volume per linac, but with 40 linacs, 2.5 X more linacs. The net result is about 3 X less total core for 6.4 X less beam energy. The smaller charge per bunch is what makes this multi-pulse small driver example require more unit core mass per kJ beam delivered than the full size 2003 design, but remember the multi-pulse format and smaller focal spot is what enables the targets for the smaller 1 MJ driver energy we are seeking.

Estimation of core loss, accelerator efficiency, and total switching power

Check: Summing beam loadings (beam energy imparted) for the bunches over cell blocks:

$$wb_{1i1} := E_{ao}(q_0, Va_{1i1}, A_0, L_{bo}, dR_{co}) \cdot Q(q_0, T_{fo}, W_{bo}, N_{bo}, N_{po}) \sum_{i1} wb_{1i1} = 4.7 \times 10^3 \quad \text{J}$$

$$wb_{2i2} := E_{ao}(q_0, Va_{2i2}, A_0, L_{bo}, dR_{co}) \cdot Q(q_0, T_{fo}, W_{bo}, N_{bo}, N_{po}) \sum_{i2} wb_{2i2} = 4.9 \times 10^3 \quad \text{J}$$

$$wb_{3i3} := E_{ao}(q_0, Va_{3i3}, A_0, L_{bo}, dR_{co}) \cdot Q(q_0, T_{fo}, W_{bo}, N_{bo}, N_{po}) \sum_{i3} wb_{3i3} = 5.1 \times 10^3 \quad \text{J}$$

$$wb_{4i4} := E_{ao}(q_0, Va_{4i4}, A_0, L_{bo}, dR_{co}) \cdot Q(q_0, T_{fo}, W_{bo}, N_{bo}, N_{po}) \sum_{i4} wb_{4i4} = 5.4 \times 10^3 \quad \text{J}$$

$$wb_{5i5} := E_{ao}(q_0, Va_{5i5}, A_0, L_{bo}, dR_{co}) \cdot Q(q_0, T_{fo}, W_{bo}, N_{bo}, N_{po}) \sum_{i5} wb_{5i5} = 5.6 \times 10^3 \quad \text{J}$$

One linac module delivers (e.g., an IRE based on this driver):

$$\sum_{i1} wb_{1i1} + \sum_{i2} wb_{2i2} + \sum_{i3} wb_{3i3} + \sum_{i4} wb_{4i4} + \sum_{i5} wb_{5i5} = 2.57 \times 10^4 \quad \text{J}$$

The small driver system example with $N_{bo} = 40$ linacs delivers a total beam energy of:

$$N_{bo} \cdot \left(\sum_{i1} wb_{1i1} + \sum_{i2} wb_{2i2} + \sum_{i3} wb_{3i3} + \sum_{i4} wb_{4i4} + \sum_{i5} wb_{5i5} \right) = 1.03 \times 10^6 \quad \text{J}$$

Now, lets turn to core losses. Lets look first at how core losses per bunch vary along the linac. The core losses per bunch per one-meter cell block assuming finemet (refer to Fig. 9-Elc3 curve):

$$wc(q, A, T_f, W_b, N_b, N_p, L_b, B_s, \eta_s, dR_c, \tau_c) := \frac{2 \cdot R_{ic}(q, A, T_f, W_b, N_b, N_p, L_b, B_s, \eta_s) \cdot dR_c + dR_c^2}{(\pi \cdot PF_r \cdot PF_z \cdot Elc3(\tau_c))^{-1}}$$

Core accel times

Core losses/bunch/cell block

J/m/bunch Eq. 22

$$\tau c_{1i1} := \tau_c(q_0, Va_{1i1}, A_0, L_{bo}) \quad wc_{1i1} := wc(q_0, A_0, T_{fo}, W_{bo}, N_{bo}, N_{po}, L_{bo}, B_{so}, \eta_{so}, dR_{co}, \tau c_{1i1})$$

$$\tau c_{2i2} := \tau_c(q_0, Va_{2i2}, A_0, L_{bo}) \quad wc_{2i2} := wc(q_0, A_0, T_{fo}, W_{bo}, N_{bo}, N_{po}, L_{bo}, B_{so}, \eta_{so}, dR_{co}, \tau c_{2i2})$$

$$\tau c_{3i3} := \tau_c(q_0, Va_{3i3}, A_0, L_{bo}) \quad wc_{3i3} := wc(q_0, A_0, T_{fo}, W_{bo}, N_{bo}, N_{po}, L_{bo}, B_{so}, \eta_{so}, dR_{co}, \tau c_{3i3})$$

$$\tau c_{4i4} := \tau_c(q_0, Va_{4i4}, A_0, L_{bo}) \quad wc_{4i4} := wc(q_0, A_0, T_{fo}, W_{bo}, N_{bo}, N_{po}, L_{bo}, B_{so}, \eta_{so}, dR_{co}, \tau c_{4i4})$$

$$\tau c_{5i5} := \tau_c(q_0, Va_{5i5}, A_0, L_{bo}) \quad wc_{5i5} := wc(q_0, A_0, T_{fo}, W_{bo}, N_{bo}, N_{po}, L_{bo}, B_{so}, \eta_{so}, dR_{co}, \tau c_{5i5})$$

Assuming an electric-->pfn efficiency $\eta_{pfn} := 0.9$

we can define local acceleration efficiency $\eta_a(\eta_{pfn}, w_b, w_c) := \frac{\eta_{pfn} \cdot w_b}{w_b + w_c}$ Eq. 23

and a local switch power per cell block $P_s(\eta_{pfn}, w_b, w_c, \tau_c) := \frac{w_b + w_c}{\eta_{pfn} \cdot \tau_c}$ (W) Eq. 24

Lets plot these quantities to see how they vary along the linac for the middle bunch:

$$\eta_{a3i3} := \eta_a(\eta_{pfn}, w_{b3i3}, w_{c3i3}) \quad P_{s3i3} := P_s(\eta_{pfn}, w_{b3i3}, w_{c3i3}, \tau_{c3i3})$$

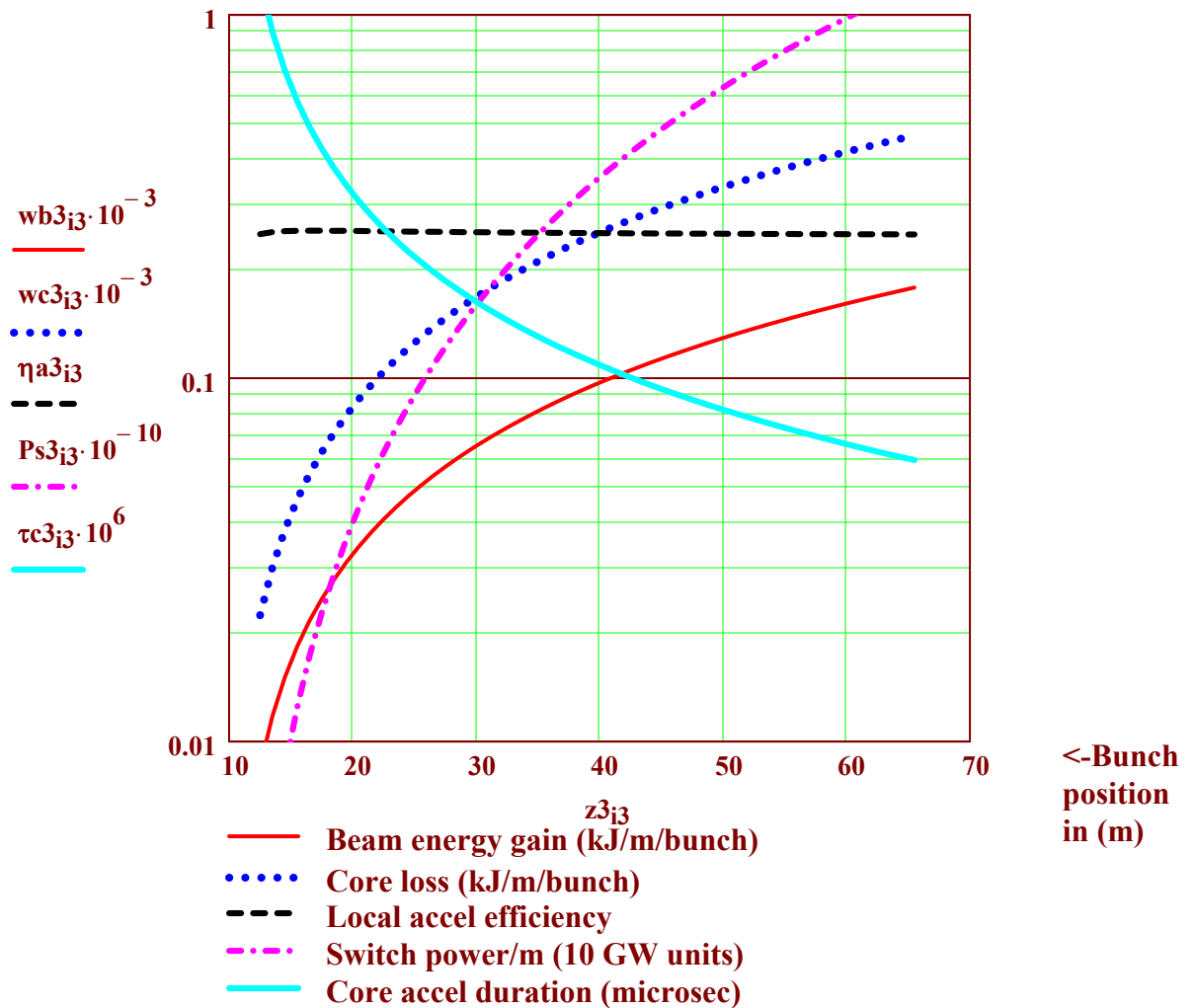


Table 19 : Local beam loading/m, core losses, acceleration efficiency, switch power and accel pulse duration as a function of distance along the linac for the middle bunch. Note acceleration efficiency relatively constant in z (η_a scales mainly $\sim w_b/m \sim Q/L_b \sim \lambda$).

The total (average) accelerator efficiency for this small driver system example:

$$\frac{\eta_{\text{pfn}} \cdot \left(\sum_{i1} \text{wb}1_{i1} + \sum_{i2} \text{wb}2_{i2} + \sum_{i3} \text{wb}3_{i3} + \sum_{i4} \text{wb}4_{i4} + \sum_{i5} \text{wb}5_{i5} \right)}{\left(\sum_{i1} \text{wb}1_{i1} + \sum_{i2} \text{wb}2_{i2} + \sum_{i3} \text{wb}3_{i3} + \sum_{i4} \text{wb}4_{i4} + \sum_{i5} \text{wb}5_{i5} \right) \dots + \left(\sum_{i1} \text{wc}1_{i1} + \sum_{i2} \text{wc}2_{i2} + \sum_{i3} \text{wc}3_{i3} + \sum_{i4} \text{wc}4_{i4} + \sum_{i5} \text{wc}5_{i5} \right)} = 0.25 \quad \text{Eq. 25}$$

Neglecting other losses as small compared to core loss, this example meets the goal of $\eta G > 10$ for target gains > 40 . This example has not been optimized, and to increase the efficiency further, one can increase the average beam line charge density/m, either by flattening the $d\lambda/dz$ profile (a uniform λ would give 2 x more efficiency compared to the $\cos^2 z$ profile in Fig. 12, or by increasing the peak λ_p , either of which increases the self field E_{bz} , in turn requiring higher average acceleration gradient also to keep $E_a > \text{self } E_{bz}$.

Switching costs should scale with total peak power installed. A fast burst of N_p -core pulses should cost not much more in switching than for the highest peak power single pulse in a pulse train (assuming modulators using optically controlled switch currents, and no extra cooling required @ low duty factor overall). Thus, the total required switch power installed is the sum of the local peak switching power requirement for each core block, set by the shortest bunch accel time for each block. The accel times scale inversely with local bunch energy/voltage, and so referring to Fig. 15, the peak switch power is set by

the tail bunch, for the first **La5 = 57** meters of linac,

by the fourth bunch between **La5 = 57** through **La4 + 6 = 62 m** **La4 = 56**

by the third bunch between **La4 + 6 = 62** through **La3 + 12 = 66 m** **La3 = 54**

by the second bunch between **La3 + 12 = 66** through **La2 + 18 = 71 m** **La2 = 53**

and by the head bunch between **La2 + 18 = 71** through **La1 + 24 = 76 m** **La1 = 52**

$$P_{s1_{i1}} := P_s(\eta_{\text{pfn}}, \text{wb}1_{i1}, \text{wc}1_{i1}, \tau_{c1_{i1}})$$

$$P_{s2_{i2}} := P_s(\eta_{\text{pfn}}, \text{wb}2_{i2}, \text{wc}2_{i2}, \tau_{c2_{i2}})$$

$$P_{s3_{i3}} := P_s(\eta_{\text{pfn}}, \text{wb}3_{i3}, \text{wc}3_{i3}, \tau_{c3_{i3}})$$

$$P_{s4_{i4}} := P_s(\eta_{\text{pfn}}, \text{wb}4_{i4}, \text{wc}4_{i4}, \tau_{c4_{i4}})$$

$$P_{s5_{i5}} := P_s(\eta_{\text{pfn}}, \text{wb}5_{i5}, \text{wc}5_{i5}, \tau_{c5_{i5}})$$

The total installed switch power sums the peak powers for the 75 core blocks/linac for $N_{bo} = 40$ linacs.

$$N_{bo} \cdot \left(\sum_{i5=1}^{57} Ps5_{i5} + \sum_{i4=51}^{56} Ps4_{i4} + \sum_{i3=50}^{54} Ps3_{i3} + \sum_{i2=48}^{53} Ps2_{i2} + \sum_{i1=47}^{52} Ps1_{i1} \right) = 2.1 \times 10^{13} \text{ W}$$

Eq. 26

The cost of switches is estimated by multiplying this figure by the asymptotic unit cost of 1000\$/GW optical drive switches (see Fig. 8):

$$UC_{sw} := 10^{-6} \text{ \$/W}$$

(same as RPD UC_{sw})

$$C_{sw} := N_{bo} \cdot \left(\sum_{i5=1}^{57} Ps5_{i5} + \sum_{i4=51}^{56} Ps4_{i4} + \sum_{i3=50}^{54} Ps3_{i3} + \sum_{i2=48}^{53} Ps2_{i2} + \sum_{i1=47}^{52} Ps1_{i1} \right) \cdot UC_{sw}$$

$$C_{sw} = 2.1 \times 10^7 \text{ \$, direct cost of switches.}$$

Eq. 27

Implicite in this switching cost is not just assuming the same low $UC_{sw} = RPD$ value here for new optical drive switches, but because the switches here can be used for N_p number of bunches.

Cost of solenoid magnets

-->assume same RPD unit costs apply to higher field Nb3Sn

$UC_{sc} := 220$ unit cost of superconducting windings.

$\rho_{wp} := 7000$ kg/m³ of superconducting windings.

The mass and cost of superconducting windings for this 1 MJ driver example is

$$M_{sc}(q, A, T_f, W_b, N_b, N_p, L_b, L_a, B_s, \eta_s) := \frac{\left[2 \cdot \frac{r_{wi}(q, A, T_f, W_b, N_b, N_p, L_b, B_s, \eta_s) \cdot B_s}{\mu_o \cdot J_{wpSn}(B_s)} \dots + \left(\frac{B_s}{\mu_o \cdot J_{wpSn}(B_s)} \right)^2 \right]}{(\rho_{wp} \cdot N_b \cdot \pi \cdot L_a \cdot PF_z)^{-1}}$$

kg. Eq. 28

$$M_{sc}(q_o, A_o, T_{fo}, W_{bo}, N_{bo}, N_{po}, L_{bo}, z1La1, B_{so}, \eta_{so}) = 1.583 \times 10^5 \text{ kg.}$$

$$C_{sc}(q, A, T_f, W_b, N_b, N_p, L_b, L_a, B_s, \eta_s) := UC_{sc} \cdot M_{sc}(q, A, T_f, W_b, N_b, N_p, L_b, L_a, B_s, \eta_s)$$

$$C_{sc}(q_o, A_o, T_{fo}, W_{bo}, N_{bo}, N_{po}, L_{bo}, z1La1, B_{so}, \eta_{so}) = 3.5 \times 10^7 \text{ \$}$$

Eq. 29

Optimizing the solenoid field

For $j := 1..17$ $B_{sj} := 2 + j$

$C_{scj} := C_{sc}(q_0, A_0, T_{fo}, W_{bo}, N_{bo}, N_{po}, L_{bo}, z1La1, B_{sj}, \eta_{so})$ superconductor cost vs B_s

$r_{wij} := r_{wi}(q_0, A_0, T_{fo}, W_{bo}, N_{bo}, N_{po}, L_{bo}, B_{sj}, \eta_{so})$ sc winding inner radius vs B_s

$r_{woj} := r_{wo}(q_0, A_0, T_{fo}, W_{bo}, N_{bo}, N_{po}, L_{bo}, B_{sj}, \eta_{so})$ sc winding outer radius vs B_s

$\eta_{aj} := \left(1 + 3 \cdot \frac{M_{mc}(q_0, A_0, T_{fo}, W_{bo}, N_{bo}, N_{po}, L_{bo}, z1La1, B_{sj}, \eta_{so}, dR_{co})}{M_{mc}(q_0, A_0, T_{fo}, W_{bo}, N_{bo}, N_{po}, L_{bo}, z1La1, 15, \eta_{so}, dR_{co})} \right)^{-1}$ accelerator efficiency

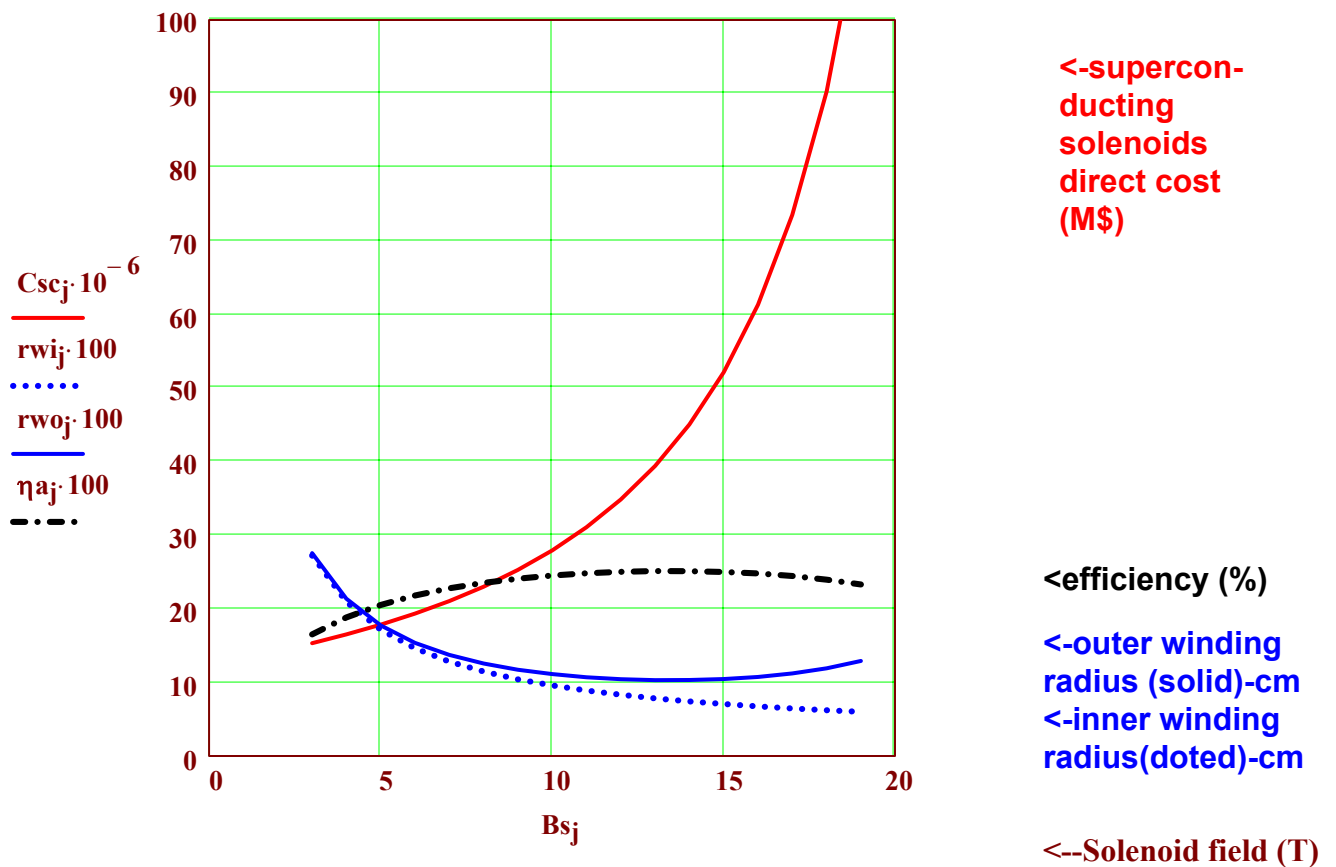


Table 20. Solenoid conductor costs for the 1 MJ small driver modular system go up with solenoid field B_s because the winding thickness increases faster than the winding radius goes down with increasing field. The outer solenoid radius actually minimizes at $B_s \sim 13$ T, where core volume and switching costs for the given 1 MJ total beam energy are minimum, and where the accelerator efficiency is maximum. Optimum field $B_s \sim 12$ T, for minimum cost.

Small 1 MJ driver cost discussion

We have not attempted so far to add up all the detailed component costs for the small 40- modular linac driver example at the RPD level, nor have we tried to optimize the many variables involved except for the solenoid field. However we have estimated the three primary component direct costs with the same unit costs (for 30 yr nth of a kind manufacturing) as was used in the RPD design: these three components together usually comprise around 50 % of the total driver direct costs of induction drivers. The purpose of trying a rough cost estimate for a small 40 linac driver system is to see if more detailed design and cost studies are warranted.

Cores @ 5 \$/kg = \$ 12 M (see pg 22 -This would triple for ferrite, but then $\eta_a > 40\%$)

Switching @ 10^{-6} \$/W = \$ 21 M

Solenoid coils @ 220 \$/kg: \$ 33 M

Cost of these three components = \$66 M direct -three major components.

Doubling this amount to account for other detailed components left out:

-->total cost ~ \$132 M all direct hardware

Multiplying by an RPD- 2.8 factor for assembly and indirect costs,

this small 1 MJ driver would have ~ \$ 370 M total driver capital cost < Demo goal

(Fig. 21 compares the RPD, the 2003 modular driver, and this small modular driver)

DEMO: Power output and CoE would depend on rep rate

(see Fig. 3 chamber concept for fast clearing)

Assuming advanced thermal conversion $\eta_{th} \sim 0.5$, gain $G = 40$ (40 MJ yield/target)

@ 6 Hz : 240 MW fusion, 120 MWe gross, 100 MWe net -->CoE ~ 6 - 8 cts/kWehr

@ 60 Hz: 2400 MW fusion, 1200 MWe gross, 1000 MWe net-->CoE~ 4 - 6 cts/kWehr

(depending on costs per target and Balance of Plant costs). Steam cycle balance of plant costs set asymptotic CoE > 2.7 cts/kWehr. Chambers designed for CFAR MHD plasma conversion could reduce BoP costs 5 X in \$/kW for thermal conversion.

(Plasma MHD conversion is another future innovation worthy to work on.)

IRE: One of the 40 driver modules

Assume one-of-a-kind units costs 4 X more than 30-yr n^{th} -of-a-kind RPD unit costs.

One module total capital cost = $4 \times 370 / 40 = \$37 \text{ M IRE}$, not counting development.

One could add > \$60 M additional for IRE supporting development (but not the prior HIF research program) and still meet the IRE goal < \$100M.

(Fig. 22 illustrates a one module IRE).

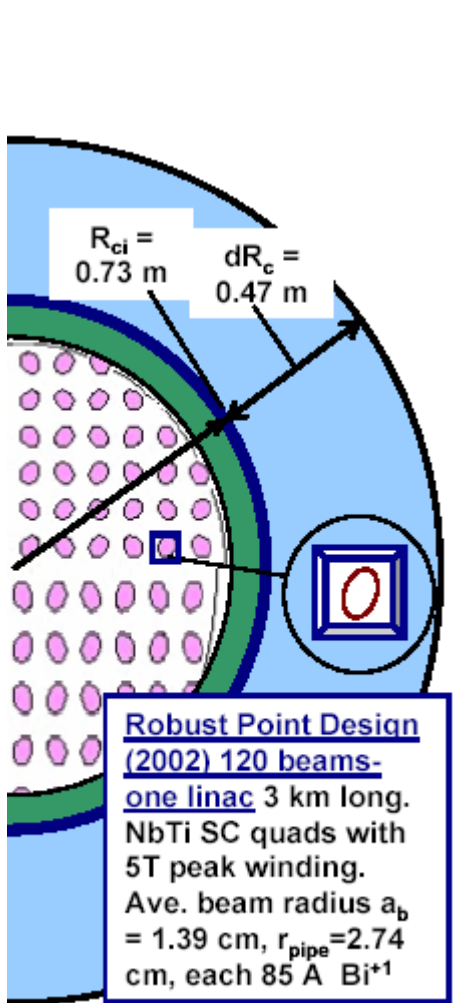
Hydrogen Plant: Increase number of linac modules to 120--> \$ 1.1 B total driver cost

Fig. 3: Gain 130 @ 3 MJ for close-coupled targets--> 400 MJ yield targets.

Increase vortex chamber (like in Fig. 4) 4X in inner radius, 3 X in outer radius

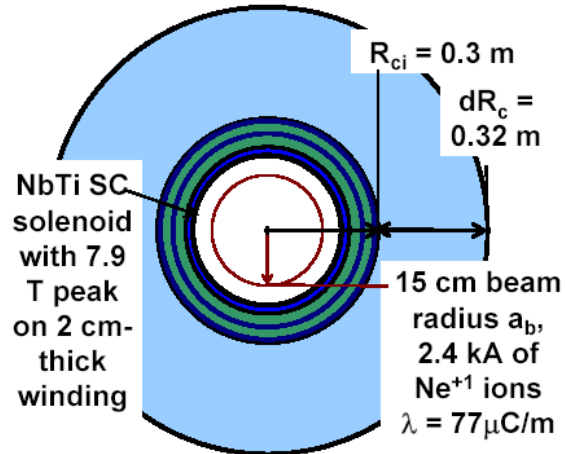
to handle 12 GW of average fusion power @ 30 Hz pulse rate -->6 GWe net for electrolysis for hydrogen fuel, and/or air conditioning to cope with global warming.

--> **Conclusion: these topics are worthy of our time for further studies.**

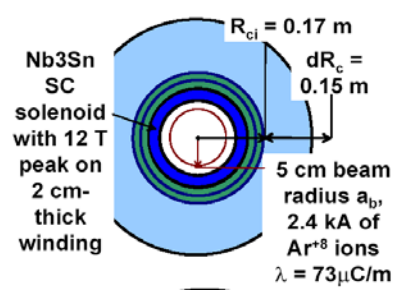


Robust Point Design (2002) 120 beams-one linac 3 km long. NbTi SC quads with 5T peak winding. Ave. beam radius $a_b = 1.39$ cm, $r_{pipe} = 2.74$ cm, each 85 A Bi^{+1}

RPD (2002) 7 MJ beam total. 35,600 tons of magnetic cores Total capital cost = \$ 2.8 B (based on detailed design)



Modular Solenoid Driver (03 summer study) One of 16 solenoid linac modules, 370 m long. Total 24 000 tons of magnetic cores, 6.4 MJ Ne^{+}



Small Modular Solenoid Driver (May-06) One of 40 solenoid linac modules, 75 m long. Total 2,400 tons of magnetic cores, 5 x 40 total pulses = total 1 MJ Ar^{+8}

Small modular, multi-pulse driver cost total capital cost = \$370 M (very rough estimate)

Fig. 21. Comparison of cross sections of recent HIF driver designs. All designs provide roughly the same range of ions in targets. The 02 and 03 designs deliver 7 and 6.4 MJ, respectively, enough for a full DRT and Hybrid target, respectively. The 06 case delivers 1 MJ for a small 40 MJ yield close-coupled target. The total lengths of the linacs in the two modular designs, if placed end-to-end, are 5.9 km for the Ne^{+1} case (large modular driver case), and 3 km for the Ar^{+8} (small modular driver) case.

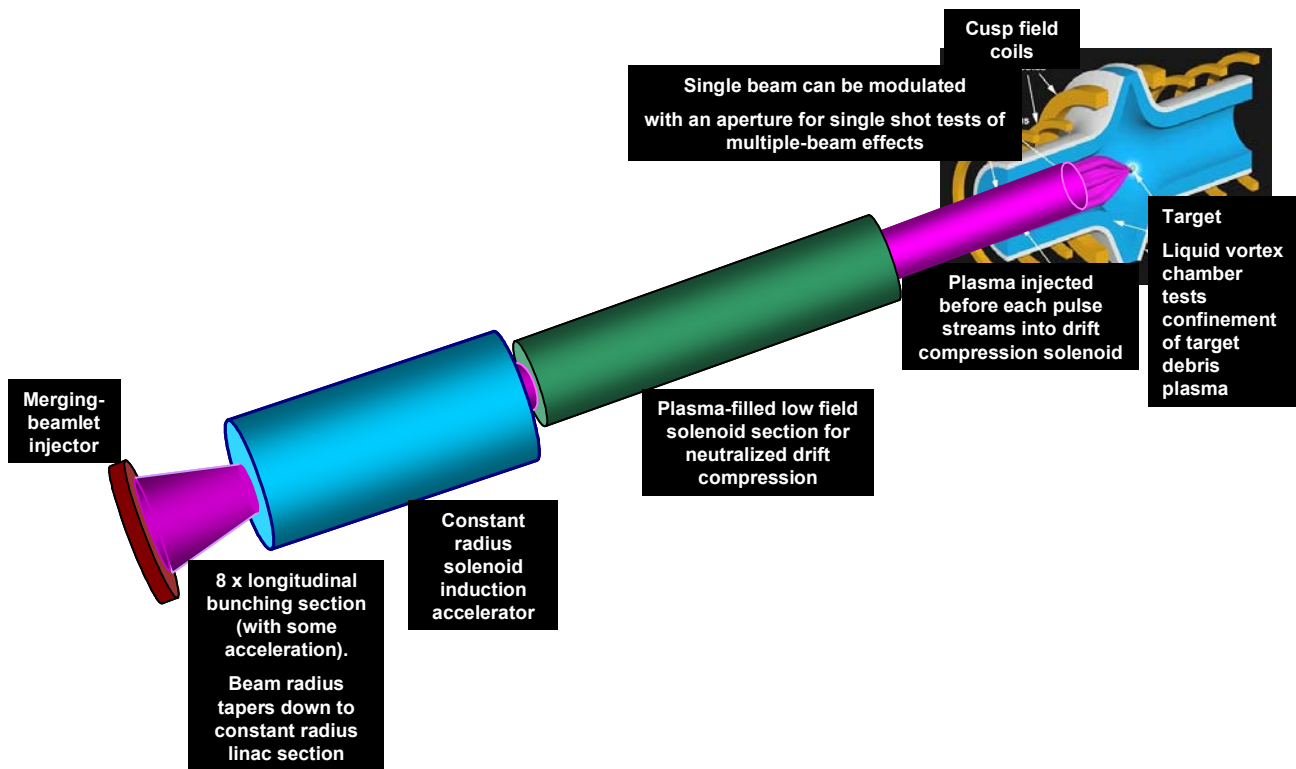


Figure 22: Concept for a single module IRE presented to Fusion Power Associates meeting, Washington DC Dec 3, 2002. That FPA meeting asked speakers to address their fusion development pathways. This IRE could be one of the 40 driver modules studied in this report, delivering 5 programmable pulses delivering a total of 25 kJ of 500 to 600 MeV Argon ions, with up to 12 TW of peak beam power for beam target interaction studies. Not shown in this IRE drawing is a fast ramping kicker needed for time-dependent focusing corrections for < 1 mm spot target experiments.